CENTER FOR TURBULENCE RESEARCH

1987 ACTIVITIES

by

Parviz Moin and William C. Reynolds

Prepared from work done under Grant

NASA-NCC-2-460

Center for Turbulence Research
Department of Mechanical Engineering
Stanford University
Stanford, California 94305

April 1988

Center for Turbulence Research--1987 activities (exlcuding the Summer Program)

Background:

The Center for Turbulence Research is a research consortium for fundamental study of turbulent flows. It is jointly operated by NASA-Ames Research Center and Stanford University. The Center became operational early in 1987 at a first year funding of $500,000.

Administrative Matters:

Currently, Parviz Moin, John Kim, and William C. Reynolds are the executive officers of the Center. Moin is the Director, Kim, the Ames coordinator, and Reynolds the program coordinator. The Center has a Steering Committee that meets regularly to act on the applications for Post-Doctoral Fellowships at the Center. The current members of the Committee are:

D. Chapman (Stanford)
S. Davis (Ames)
J. Kim (Ames)
P. Moin (Ames/Stanford)
W. Reynolds (Ames/Stanford)
M. Rubesin (Ames)

The Center also has a high level Advisory Committee that meets annually and reviews the Center's activities and accomplishments. The Committee members represent government, industry, and academia. The the names of the Advisory Committee members are attached. Their first meeting took place on March 20-21, 1988. The chairman of the Committee reports its findings to the Center for Turbulence Research officers, to the Ames Director, and to the Director of Aerophysics.

An office assistant (Susan Hinton) was hired on February 1 to help with administrative matters.

Technical Activities:

The following provides a chronology of the events and individuals who participated in CTR. The individuals listed were appointed before December 1, 1987.

Dr. Tsan Shih was appointed (on April 1) as a Post-doctoral Fellow. Dr. Shih's speciality is turbulence modeling and specifically, one point closures. He has worked closely with Nagi Mansour of Ames utilizing the direct numerical simulation databases for testing turbulence models. He is currently working on the near wall behavior of turbulence models. Shih, on partial support from Air Force Office of Scientific Research, has been working with Parviz Moin on modeling of three-dimensional turbulent boundary layers. He has carried-out simulations and documented the statistical behavior of the channel flow subjected to imposition of pressure gradient or shear in the transverse direction. He is currently computing the Reynolds stress budget in this flow.

Dr. Laurence Keefe (June 1987-Nov. 1987) has continued his work at Ames to measure the dimension of an attractor in low Reynolds number turbulent channel flow. Since December 1 he has been supported by AFOSR. The overall objective is to study the relevance and implications of the dynamical systems theory to open turbulent flows.

Dr. Kevin Thompson (June 1987-present) (1/3 CTR support, 2/3 Ames' Space Science Division) is studying turbulence in the early solar nebula. In this environment, turbulence is subjected to stratification, variable gravity, variable (Keplerian) rotation, and heat sources and heat loss by radiation. Thompson is currently writing and testing a code for simulation of compressible turbulence in three-dimensions.

Dr. Julian Hunt (July 1987-August 1987)(Cambridge Univ.) spent an additional month beyond the summer program to continue work on space time correlations in homogeneous turbulence, on sel-similarity of two-point correlations in boundary layers, and on rapid distortion theory of near wall turbulence.

Professor Paolo Orlandi (July 1987-Oct. 1987) continued the work on development of an accurate finite-difference code for simulation of incompressible Navier-Stokes equations in generalized geometries during three of his four months' stay. The code is now tested for several well known laminar cases, and should be completed during Prof. Orlandi's visit in the summer of 88.

Professor C. Benocci (Sept. 14, 1987-Oct. 10, 1987) is an assistant professor at the von Karman Institute in Brussels. His objective was to test phenomenological models for Lagrangian statistics using direct numerical simulation of forced isotropic turbulence. Although the generality of the results were hampered by the low Reynolds numbers in the simulations, some new results emerged. In particular, it was shown that contrary to the earlier assumptions, Lagrangian and Eulerian velocity auto-correlation are quite close to each other. Moreover, the autocorrelation curve does not exhibit the exponential shape in contrast to the solutions to the commonly used Lagrangian (Longevin) equation. It should be noted that Benocci used a 32x32x32 simulation at very low Reynolds numbers, and these results should be reexamined with higher resolution and Reynolds numbers.

Dr. James Broadwell (Oct. 87-Dec. 87) is a Sr. scientist at Cal-Tech. He is working closely with M. Rogers and R. Moser at Ames. The objective is to test Broadwell's model for mixing. This model is based on organized structures in shear flows. This work has led M. Rogers to develop a new code for time-developing mixing layer and jets and is a key element for CTR's plans for strengthening the combustion and reacting flow research.

Professor N. Etemadi (September 1987-August 1988) (1/3 CTR support, 2/3 Univ. of Illinois) is a mathematician from University of Illinois in Chicago. His field of speciality is Probability Theory. His appointment was based on the Center's goal of generating new ideas in turbulence research. Prof. Etemadi has had no prior knowledge of fluid mechanics or turbulence. He has used the first half of his sabbatical in studying classical turbulence and turbulence terminology. It is expected that in the second half he will apply his expertise in probability theory to turbulence.

Dr. George Karniadakis's (Oct. 1987-February 1988) speciality is in application of spectral element method to flows in complex geometries. During his tenure at CTR the objective was to apply the Spectral Element Method to direct simulation of turbulence on a wall with riblets. It has been determined experimentally that the flow over such a wall has reduced skin friction despite the increase wetted area. To this end, the laminar flow over a triangle was computed, for code validation and the results compared well with the experimental results. The 2-D spectral element code was modified to three dimensions and preliminary runs for the channel with riblets is initiated. It is expected that these calculations will be continued by Dr. Karniadakis at MIT, and a graduate student will continue the work at CTR.

Drs. Thomas, R. Osborn and Dr. Hidekatsu Yamazaki (Oct. 16, 87-Nov. 16 87). The objective of these oceanographers from The Johns Hopkins University was to study encounter rates between planktonic particles in a turbulent fluid. The application is to the food web of oceanic plankton. Random walk was used to model planktonic motion relative to the turbulent flow environment which was simulated with a 64x64x64 calculation of forced isotropic turbulence. As expected, for the cases with least energetic random walks, turbulence increased the contact rates between prey and predator, and with the most energetic random walks, effect of turbulence was negligible. The results to date are very preliminary. The work is being continued at Johns Hopkins, and it is hoped that its eventual dissemination will attract other oceanographers to CTR.

Dr. Moon J. Lee (Nov. 1987-present) will continue his work on analysis of the effects of shear on turbulence. A simulation of a shear-free turbulent boundary layer is planned to complement the homogeneous shear flow simulations.

Dr. Jonathan Watmuff (Nov. 1987-present) will conduct an experimental investigation of turbulent boundary layers with adverse pressure gradient. The objective is to test the limits of Spalart's assumptions in his direct numerical simulation code. Dr. Watmuff will bring a great deal of expertise in flow instrumentation to Ames' Fluid Mechanics Laboratory.

Graduate Student Research Assistants:

P. Beaudan (Oct. 1987-) 25% RA. Spectral Element Method for complex geometries.

J. Neves (Oct. 1987-March 1988) 50% RA. Numerical simulation of an axial-flow over a cylinder. J. Neves will be supported by Office of Naval Research, starting April 1, 1988.

S. Sorakayalpet (Oct. 1987-March 1988) 25% RA. Space-time characteristics of wall-pressure fluctuations. S. Sorakayalpet will continue on an ONR contract.

K. Squires (Oct. 1987-Sept. 1988) 50% RA. Effect of particle loading on turbulence structure and modeling.

M. Plesniak (Jan. 1988-June 1988) Experimental study of the effects of longitudinal curvature on mixing layers.

M. Woronowicz (July 1987-Sept. 1987) This study was sponsored by CTR during the summer of 1987 to determine whether particle simulation could be used to study low-speed turbulence. The method has been developed by Baganoff to simulate hypersonic flows. Several standard laminar flows were simulated with moderate success. This involved developing methods to measure such quantities as kinematic viscosity from the particle simulations. Due to some anomalies in laminar flow calculations, no attempt was made to simulate turbulent flows. Presently, CTR has no plan to continue supporting this effort.

APPENDIX 1

Report by C. Benocci

Lagrangian Statistics in Homogeneous Isotropic Turbulence: Comparison Between Direct Numerical Simulation and Random Flight Models

By C. Benocci[1]

[1] Institut von Karman de Dynamique des Fluides

Lagrangian techniques have found widespread application to the prediction and understanding of turbulent transport phenomena (Monin and Yaglom) and have yielded satisfactory results for different cases of shear flow problems (Durbin, 1983). However, it must be kept in mind that in most experiments what is really available are Eulerian statistics (Monin and Yaglom), and it is far from obvious how to extract from them the information relevant to the Lagrangian behavior of the flow; in consequence, Lagrangian models still include some hypothesis for which no adequate supporting evidence was up to now available. Direct numerical simulation of turbulence offers a new way to obtain Lagrangian statistics and so verify the validity of the current predictive models and the accuracy of their results. After the pioneering work by Riley (Riley and Patterson, 1974) in the 70's, some such results have just appeared in the literature (Lee et al, Yeung and Pope). The present contribution follows in part similar lines, but focuses upon two particle statistics and comparison with existing models (Durbin, 1980, Sawford and Hunt, 1985).

1.The classical Lagrangian model

In Lagrangian modeling, turbulent transport phenomena are simulated by the motion of "fluid particles." The fundamental variables are the position of the particle $\tilde{X}(\tilde{x},t)$, where $\tilde{x}$ is the initial point of the trajectory (release point) and its velocity $\tilde{V}(\tilde{x},t)$. Another quite useful quantity is the displacement vector $\tilde{Y}(\tilde{x},t)$ defined as:

$$\tilde{Y}(\tilde{x},t) = \tilde{X}(\tilde{x},t) - \tilde{x}$$

Reynolds decomposition can obviously be applied to those quantities, giving, for example

$$\tilde{V}(\tilde{x},t) = \overline{\tilde{V}}(\tilde{x},t) + \tilde{V}'(\tilde{x},t)$$

From X, Y, and V the relevant statistical information could be extracted, the most important being the fluctuating displacement covariance tensor:

$$D_{ij}^{(L)}(t) = \overline{Y_i'(t)Y_j'(t)}$$

the fluctuating velocity covariance tensor:

$$B_{ij}^{(L)} = \overline{V_i'(\tilde{x},t)V_j'(\tilde{x},t)}$$

and the Lagrangian integral time scale:

$$T^{(L)} = \int_0^\infty R_{ii}^{(L)} dt = \int_0^\infty \frac{\overline{V_i'(\tilde{x},t)V_i'(\tilde{x},o)}}{\overline{V_i'^2(\tilde{x},t)}^{1/2}\overline{V_i'^2(\tilde{x},o)}^{1/2}} dt$$

where $R_{ii}^{(L)}$ is the velocity autocorrelation. Dimensional and theoretical analysis (Monin and Yaglom) show that:

$$D_{ij}^{(L)}(t) \sim t^2 \qquad t << T^{(L)}$$

$$D_{ij}^{(L)} \sim t \qquad t >> T^{(L)}$$

more refined formulations can be obtained, for simple flows only making assumptions about the shape of the autocorrelation function $R_{ii}^{(L)}$. The latter is generally (Lee et al) assumed to have an exponential form:

$$R_{ii}^{(L)}(t) = e^{-t/T_{ii}^{(L)}}$$

Using the form above, an analytical relationship can be found for the 2nd order moments on the displacement (the trace of the displacement covariance tensor) for the case of homogeneous stationary turbulence:

$$D_{ii}^{(L)}(t) = 2\overline{u'_i}^2 T_{ii}^{(L)}\left(\frac{t}{T_{ii}^{(L)}} - 1 + e^{-t/T_{ii}^{(L)}}\right)$$

where u'_i is the fluctuating Eulerian velocity and $T_{ii}^{(L)}$ must still be determined. To this end, it has generally been assumed that the Lagrangian autocorrelation be stronger than the Eulerian one, and a linear relationship of the type:

$$R_{ii}^{(L)}(t) = R_{ii}^{(E)}(\beta t)$$

has often been used ($\beta \simeq .4$ for the atmospheric surface layer). However, in the first numerical results (Riley and Patterson, 1974), the size and shape of the Lagrangian and Eulerian correlations were actually quite close. A similar trend is also shown by the most recent tests (Lee et al) for homogeneous decaying turbulence. In view of this discrepancy between theory and available numerical results, investigation of the Lagrangian velocity autocorrelation and time scale is the most urgent task of direct numerical simulation.

2. The random walk model of Lagrangian transport

Simplified relationships of the type presented in the previous section are available only for some very simple cases of turbulent flow; for all the others, numerical solutions have to be sought. To this end, the turbulent Eulerian velocity field is taken as a random process and replaced by a known stochastic process of similar statistics. For a turbulent flow having a finite time scale and high turbulent Reynolds number, it is assumed that the turbulent acceleration is uncorrelated and can be simulated with a Gaussian random walk process. Under this hypothesis, the infinitesimal change of Lagrangian velocity dv over the time dt is given by the Lagrangian equation (Durbin, 1983):

$$dV_i = -\frac{V_i}{T_{ii}^{(L)}}dt + \left(\frac{2\overline{u_i'^2}}{T_{ii}^{(L)}}\right)^{1/2} dW_t$$

where dW_t is a step in a random walk process having a Gaussian pdf of mean 0 and variance dt. The Lagrangian equation automatically imposes the exponential form of the Lagrangian autocorrelation. In practice a discrete process is used and the particle is advanced in time with an explicit technique:

$$X_i^n = X_i^{n-1} + V_i^{n-1}\Delta t$$

$$V_i^n = V_i^{n-1} + \Delta V_i$$

where n is the current time step. The above technique has two main weak points: the first lies in the fact that the trajectory of each particle is generated by an independent random process and is, therefore, *entirely* uncorrelated with respect to other trajectories, while in reality particles moving in a *correlated* Eulerian velocity field have to be correlated with each other; the second (and related) is that the velocity field so generated does not respect continuity. The first difficulty is removed by two

particle models (Durbin, 1980, Sawford and Hunt, 1985) where the basic "event" is the correlated motion of one pair of particles. The two particles are moved with a law of the type:

$$dX_1 = (\alpha U' + \beta U'')dt$$

$$dX_2 = (\alpha U'' + \beta U')dt$$

where α and β are functions of the pair separation S, defined as (Durbin, 1980):

$$S = \frac{X_1 - X_2}{2^{1/2}}$$

and the Lagrangian length scale:

$$L = (\overline{u'^2})^{1/2} T^{(L)}$$

while the U′ and U″ velocities are respectively:

$$U' = \frac{V_1 + V_2}{2^{1/2}} \qquad U'' = \frac{V_1 - V_2}{2^{1/2}}$$

V_1 and V_2 being generated through two independent random processes obeying the Lagrangian equation. The issue of continuity can be addressed only by treating reverse dispersion problems (Sawford and Hunt, 1985) (i.e. finding the source which corresponds to a given marker's distribution). This makes the approach unpractical for real prediction work. Comparison with direct numerical simulation should give an evaluation of the size of the errors due to the unphysical features of the velocity fields.

3. Direct simulation of Lagrangian motion

In this initial phase,the study of Lagrangian statistics was limited to the case of isotropic homogeneous stationary turbulence with no mean velocity. The corresponding Eulerian velocity field was generated with the Rogallo code (Lee and Reynolds, 1985); stationarity in absence of a mean shear gradient was achieved by adding a forcing term on the lowest wavenumber. Most of the simulations made were for a 32^3 mesh. The relevant quantities of the Eulerian flowfield are:

$\nu = 0.1$

$\overline{u'^2} = 2.25$ (deviation 5%)

$\varepsilon = 8.5$

Therefore, the Kolmogorov microscale is:

$$\eta = (\frac{\nu^3}{\varepsilon})^{1/4} = 0.104$$

and the Taylor microscale:

$$\lambda = (15\overline{u'^2}\,\frac{\nu}{\varepsilon})^{1/2} = 0.945$$

corresponding to a turbulence Reynolds number $R_\lambda e = 21.26$. The separation between the two scales is, therefore, too small for the existence of a developed inertial subrange. The theoretical relationship:

$$L^{(E)} = \frac{A}{15}\lambda Re_\lambda$$

gives a value of 1.07 for the Eulerian macroscale $L^{(E)}$ compared to about 1.25 for the simulation. The turbulent Reynolds number based upon the length scale lies therefore in the 25–30 range. It has

to be remarked that the effect of the forcing is to introduce a large scale perturbation which cannot be removed from the results: the Eulerian correlation does not, therefore, go down to 0 (Figure 1), and the overall concept of macroscale remains vague. Before passing to the analysis of the results, it must be remarked again that the Lagrangian equation model requires the turbulent acceleration to be uncorrelated i.e. the acceleration time T_a scale to be much smaller than the velocity one, as:

$$T_a \simeq (Re_L)^{-1/2} T^{(L)}$$

This given for the present simulation:

$$T_a \simeq 0.2 T^{(L)}$$

We are, therefore, at the very limit of the region of applicability of the model. The results of the present comparison cannot, therefore, be taken as final until confirmed by tests at higher Re's.

4. Influence of the number of markers

The 32^3 simulations were run with 4,096 particles; the number was chosen to keep the CPU time requirement to a manageable amount ($\simeq$ 5 sec per time step). As stochastic methods are relatively slow to converge (error size decreases with $N^{-1/2}$ where N is the number of events), the first task was to verify whether the sample was good enough to give reliable results. To this end the full results were compared with the ones obtained by sampling one "event" (particle or pair of particles) out of two and out of four. Some relevant comparisons are presented in Figure 2 in the form of relative difference between the two results, i.e.:

$$\text{output} = \frac{\text{Result 1} - \text{Result 2}}{(\text{Result 1} + \text{Result 2})/2}$$

Figure 2 compares the predicted 2nd order moment of the displacement of single particles for 4,096 and 2,048 event: maximum relative error is less than 10^{-3}, showing that the present distribution is adequate for single particle statistics. Figure 3 show the same comparison for the second order moments of the separation of a pair of particles (2,048 versus 1,024) events) and the increase in error is quite visible for small separation times; where the effect of the initial position of the marker is felt; for separation times higher than $2(\simeq 4T^{(L)})$, the error is still low. As can be expected, much higher errors will be encountered when considering the separation velocity $w = ds/dt$, which is computed numerically from the separation; the separation velocity rms difference is shown in Figure 4. It can be seen from the figure that differences are of the order of 10^{-1} Therefore, results for the separation velocity are to be considered as qualitative only. Reducing again by half the number of samples, the errors increase by nearly one order of magnitude. It is somewhat surprising to find good convergence with so limited a number of events (most two particle simulations use 10^4 events (Sawford and Hunt, 1985)). This is due to the fact that the sample is still generated from a correct velocity field.

5. Influence of the initial distribution

As previously mentioned, two tests were performed: the first case used a separation between markers of order of 2Δ and the second case used a separation of the order of Δ. Consistent with the effect of the number of markers on the results, differences in single-particle statistics between cases using different initial distributions were negligible. Differences in two-particle statistics, however, are affected by the initial distribution, with the difference becoming negligible after the particles motion becomes uncorrelated (Figure 5). In conclusion, the two cases can be used indifferently to discuss all the statistics with the exception of the ones related to separation.

6. Single particle Lagrangian statistics

As it was shown in a previous paragraph, the present simulations 1 and 2 can be taken to represent fully converged and equivalent solutions of the Lagrangian problem as far as one particle statistics are concerned. Therefore, all the pertinent data will be examined together in the present paragraph.

Based upon the average of six results (3 components * 2 cases), the Lagrangian time scale takes the value:

$$T^{(L)} = 0.526$$

with a 5% dispersion for individual data. The corresponding length scale L is given by:

$$L = \overline{(u'^2)}^{1/2} T^{(L)} = 1.18$$

quite close to the value of the Eulerian macroscale (see paragraph 4). The present results, therefore, agree with the previous ones (Riley and Patterson, 1974, Lee et al, Yeung and Pope) in indicating that the Lagrangian and Eulerian correlations are quite close. Whether these results are of general value or are due to the low Reynolds number of the simulation is an open question which can only be answered by further tests. A remarkable result of the present tests is the discrepancy between the computed Lagrangian autocorrelation and the theoretical exponential shape (Figure 6). It can be shown that the numerical solution of the Lagrangian equation will yield the exponential form for the autocorrelation. Similar trends are made evident by a comparison of the displacement p.d.f. (Figure 19). As an obvious consequence, the results of the direct simulation do not fit well with the already discussed theoretical results:

$$\overline{Y'}^2 = 2\overline{u'^2}\, T^{(L)2}\left(\frac{t}{T^{(L)^2}} - 1 + e^{-t/T^{(L)}}\right)$$

for the 2nd order moment of the displacement. As it can be observed in Figure 8, the numerical results diverge from the previous relationship as soon as the initial development $\overline{Y'}^2 \sim t^2$ is over, and become parallel to the theoretical curve only for $t > 16T^{(L)}$. By contrast, the numerical solution of the Lagrangian equation fits the theory perfectly (Figure 9). To conclude, it must be remarked again that the present calculations have been made at the very lowest edge of the Reynolds number region where the Lagrangian equation can be applied, and, therefore, the above discussed results are not enough to draw a conclusion upon the overall validity of the model. Surely it draws the attention over a quite peculiar behavior of the Lagrangian variables at low turbulent Reynolds numbers and puts in evidence the need for both tests at higher Re and further tests in the same range to develop a suitable understanding of such a regime.

7. Two particle statistics

As it was already remarked, the statistics of a pair of particles are potentially the ones most important for the understanding of the Lagrangian phenomenology. However, the results reported here can only be regarded as preliminary in nature. It has already been observed (paragraph 5) that the number of "events" (about 2,000) is still low and the convergence of the results not yet complete. Moreover, the prediction appears to be strongly affected by the nature of the forcing. This can be remarked by comparing the separation average velocity obtained from the direct prediction (Figures 10) with that corresponding to the two particle random flight model (Figures 11). It can clearly be seen that the patterns of the mean velocities are quite different; the ones predicted by the Lagrangian equation decrease in time (for large separation times) with a law which is smooth enough (considering the relatively limited number of markers) and filling the expected $z^{-1/2}$ law. On the contrary, the direct simulation yields a profile containing consecutive peaks, more or less in correspondence with the peaks of the Eulerian correlation (Figure 1). It appears that at large times when the two elements of the pair are far away and their relative motion is dominated by the energy carrying eddies, the influence of the forcing becomes dominant. Consequently, large differences exist between the separation predicted by the direct simulation and the Lagrangian equation. As an example, the 2nd order moments are shown for the direct simulation in Figure 12 and for the two particle model in Figure 13. The differences are evident, above all in the initial part where the behavior of the mean separation velocity is entirely different. Unfortunately the only available theoretical prediction of the separation moments is valid only for high turbulent Re and assumes, above all, the existence of an inertial subrange. Therefore, its predictions are, unsurprisingly, far from the numerical results (Figure 14).

8. Conclusions

The present report is only a first *quite preliminary draft* covering some of the results obtained during the stage of the author at the Center for Turbulence Research. Another part of the results has not yet been processed and will be discussed in the forthcoming second draft. Tentative conclusions are:

- It is confirmed that Eulerian and Lagrangian macroscales are of the same size, at least in the range of turbulent Reynolds number which can, at present, be tackled by direct simulation.
- The predicted autocorrelation has no negligible differences with respect to the expected exponential shape.
- One particle statistics can be analyzed in detail using the present results, but two particle statistics require more "events" (double at least) and a better understanding of the influence of forcing upon the large scales.
- Turbulent Reynolds numbers at least 4 times higher than the present one should be reached to fulfill all the aims of the present investigation.

9. Acknowledgements

The author thanks the Center for Turbulence Research for supporting the present investigation, and Mr. K. Squires and Prof. P. Moin for their assistance and technical advice. Finally, the most sincere thanks to Ms. Debra Spinks for trying to make sense of the author's handwriting!

REFERENCES

MONIN AND YAGLOM Statistical Fluid Mechanics. *MIT Press.*

DURBIN 1983 Stochastic differential equations and turbulent diffusion . *NASA RP.* , 1103.

RILEY AND PATTERSON 1974 Diffusion experiments with numerically integrated isotropic turbulence. *Physics of Fluids.* **Vol. 17,** 292-97.

LEE ET AL Study of lagrangian characteristic times using direct numerical simulation of turbulence. *6th Symposium Turbulent Shear Flows.*

YEUNG AND POPE Lagrangian velocity statistics obtained from direct numerical simulation of homogeneous turbulence. *6th Symposium Turbulent Shear Flows.*

DURBIN 1980 A stochastic model of two-particle dimension and concentration fluctuations in homogeneous turbulence. *JFM* . **Vol. 100,** 273-302.

SAWFORD AND HUNT 1985 Effects of turbulence structure, molecular diffusion and source size on scalar fluctuations in homogeneous turbulence. *JFM.* **Vol. 165,** 373-400.

LEE AND REYNOLDS 1985 Numerical experiments on the structure of homogeneous turbulence. *Stanford University Report TF-24.*

Eulerian Autocorrelations

Average over 4096 positions

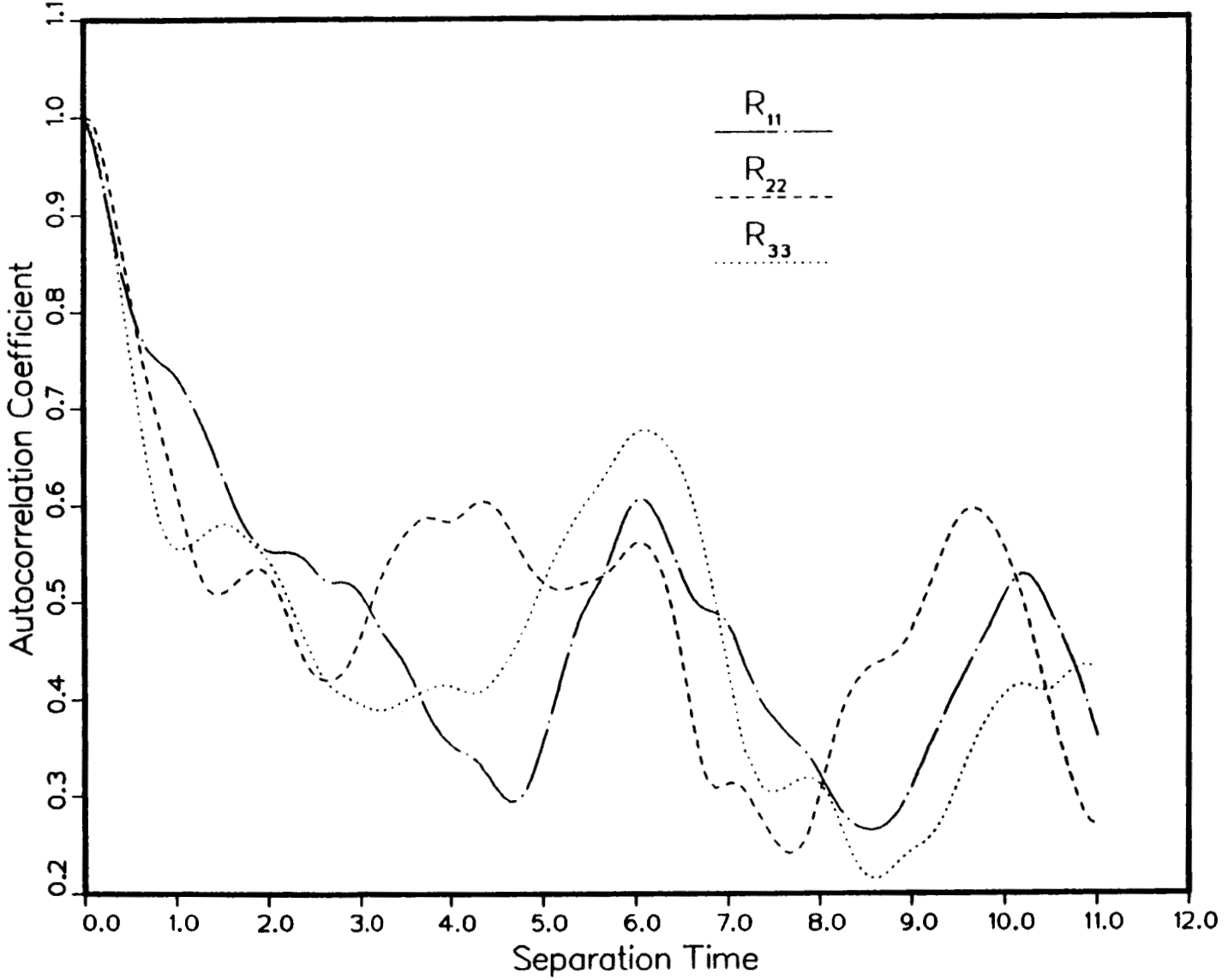

Figure 1

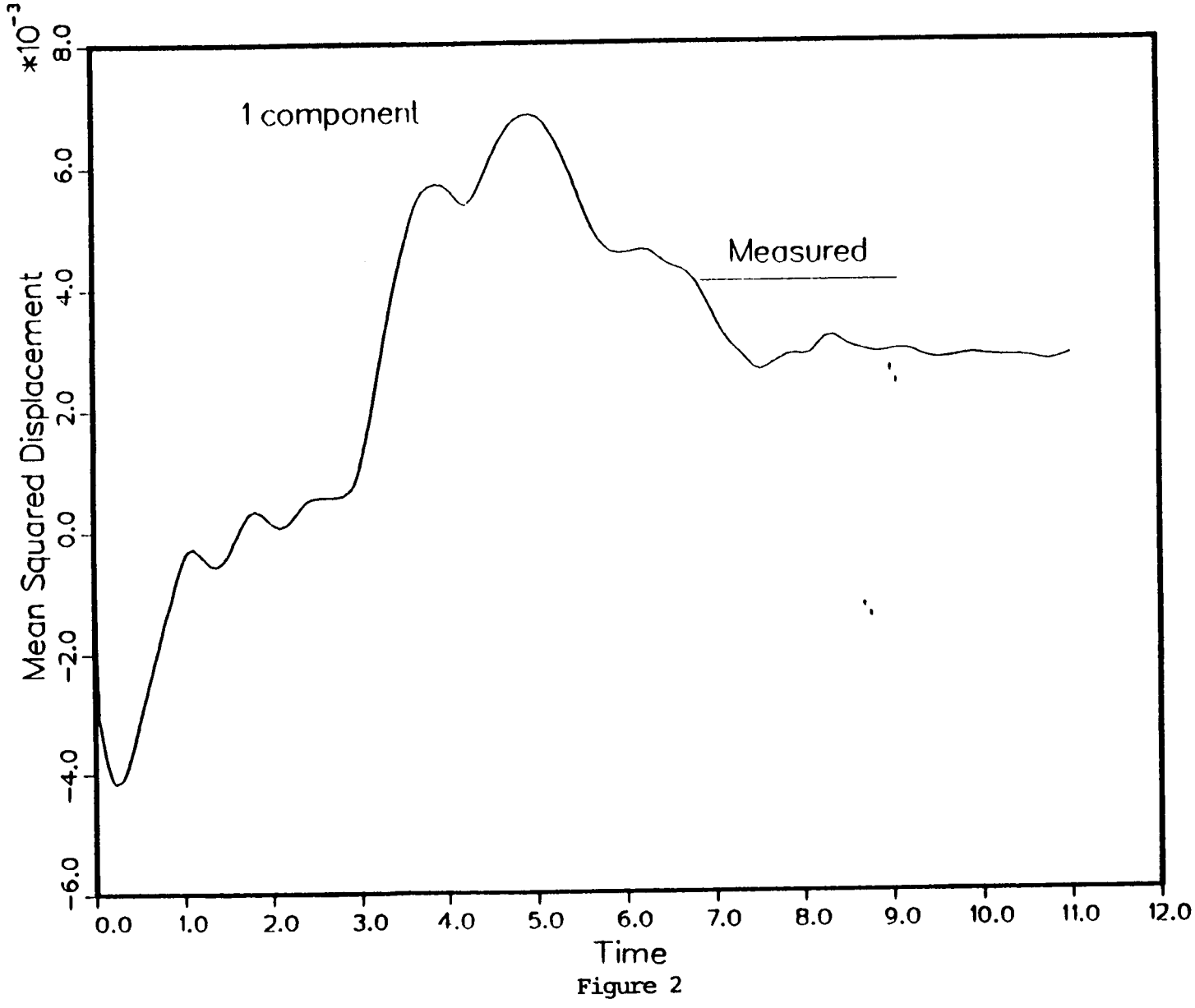

Figure 2

Separation variance of a pair dAverage over 4096 particles

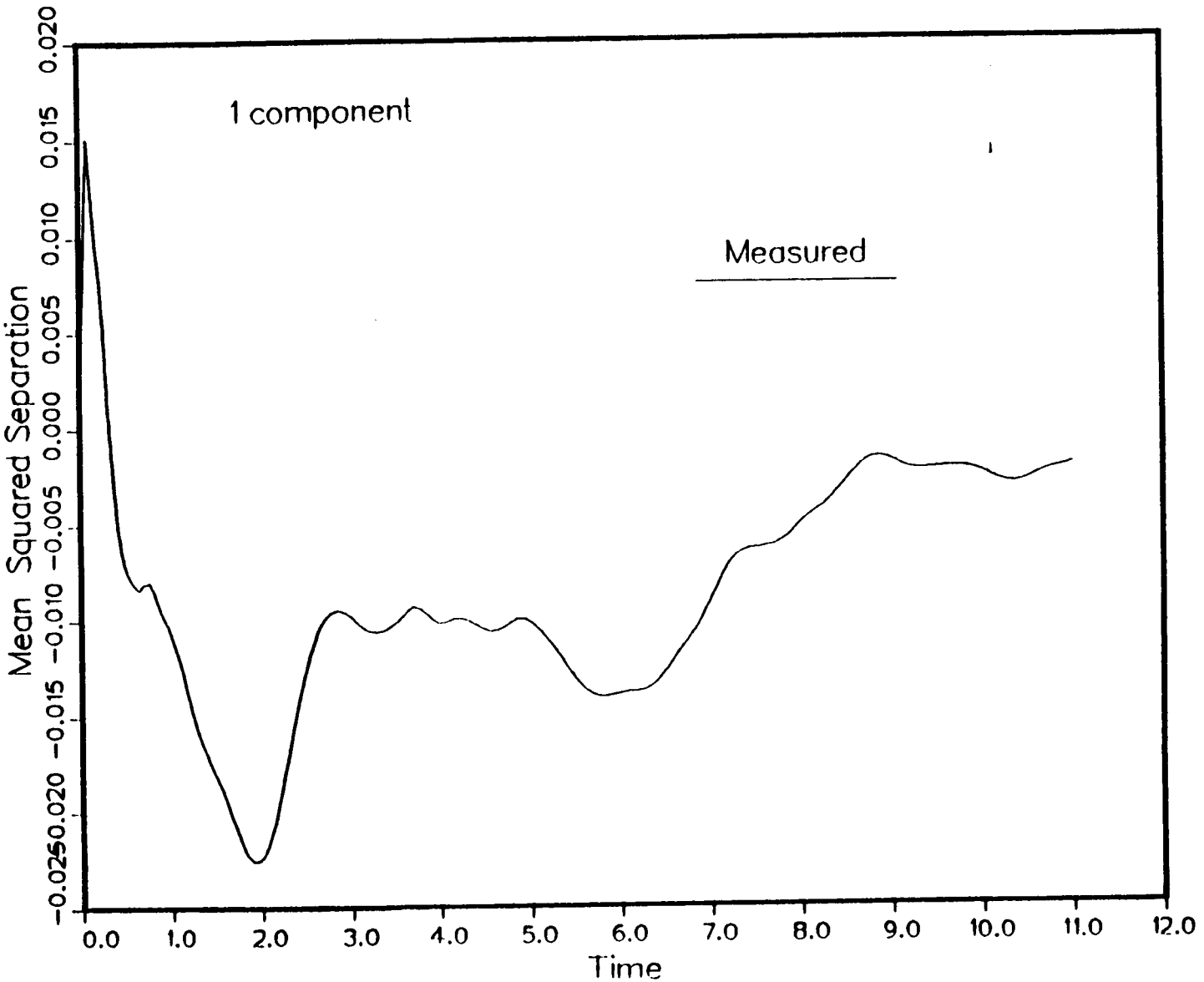

Figure 3

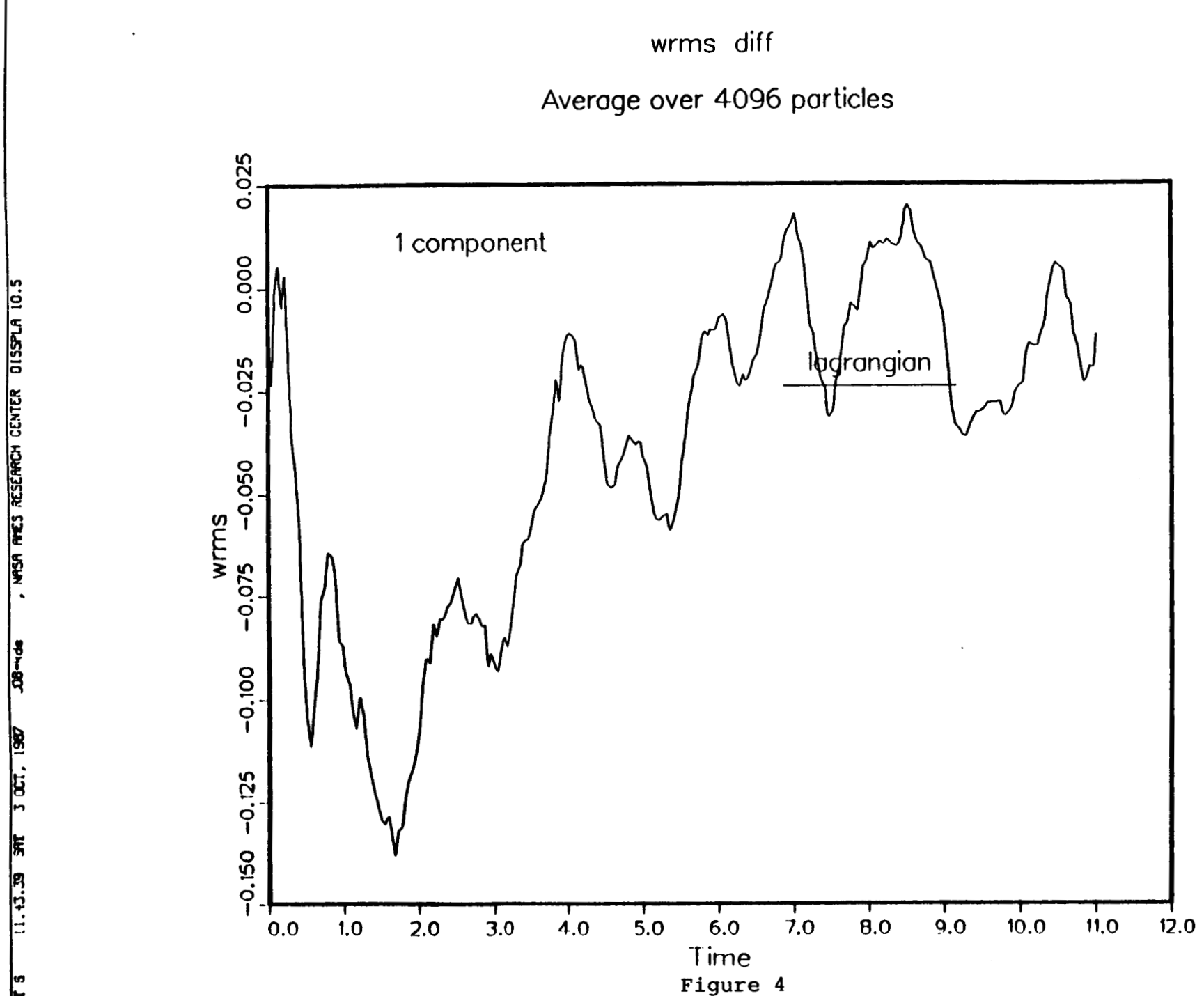
wrms diff
Average over 4096 particles
1 component
lagrangian
wrms
0.025
0.000
-0.025
-0.050
-0.075
-0.100
-0.125
-0.150
0.0
1.0
2.0
3.0
4.0
5.0
6.0
7.0
8.0
9.0
10.0
11.0
12.0
Time
PLOT 6 11:43.39 SAT 3 OCT, 1987 JOB=ide , NASA AMES RESEARCH CENTER DISSPLA 10.5

Figure 4

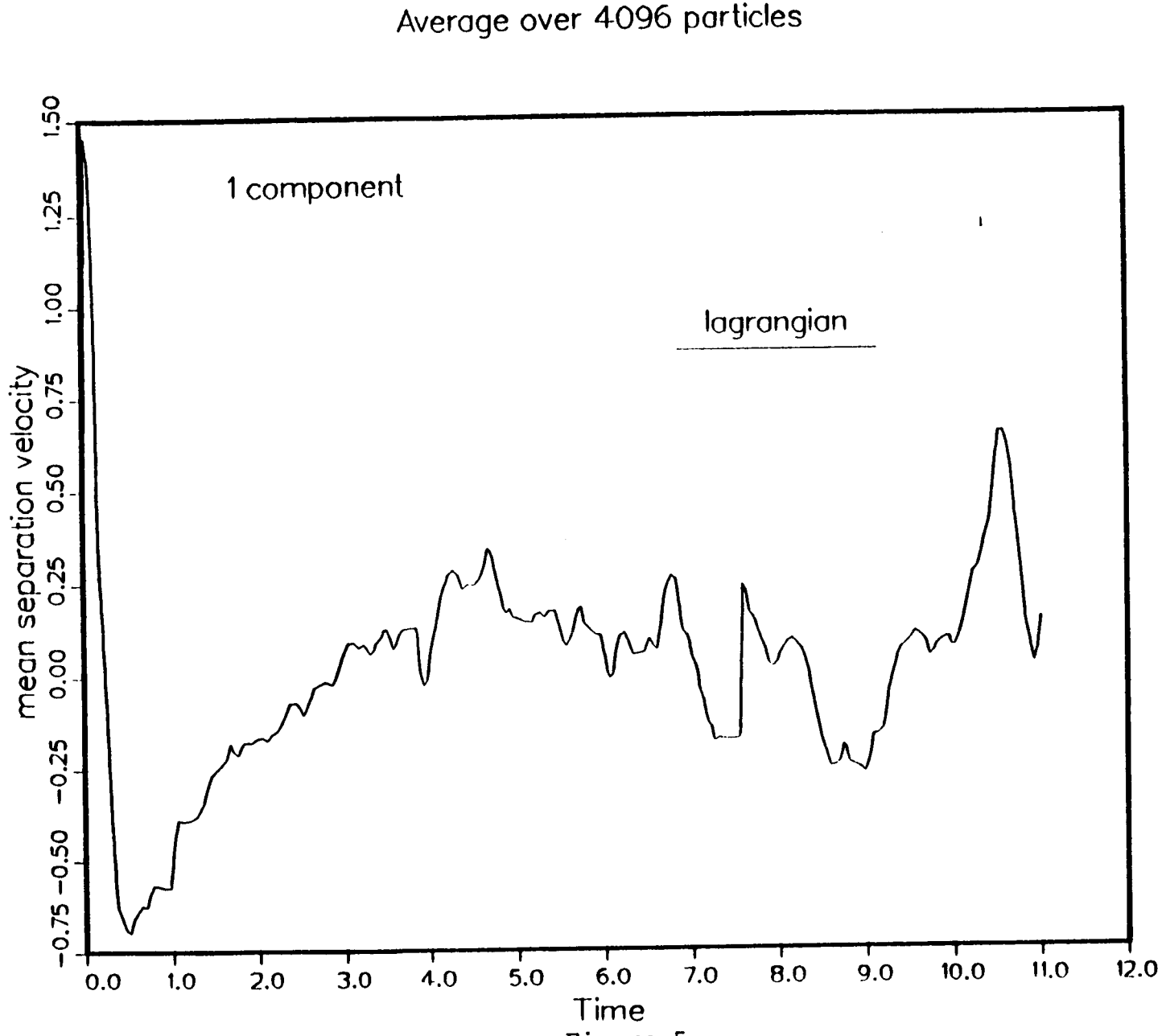
mean separation velocity diff
Average over 4096 particles
1 component
lagrangian
mean separation velocity
1.50
1.25
1.00
0.75
0.50
0.25
0.00
-0.25
-0.50
-0.75
0.0
1.0
2.0
3.0
4.0
5.0
6.0
7.0
8.0
9.0
10.0
11.0
12.0
Time

Figure 5

Autocorrelation Comparison NN

Average over 4096 particles

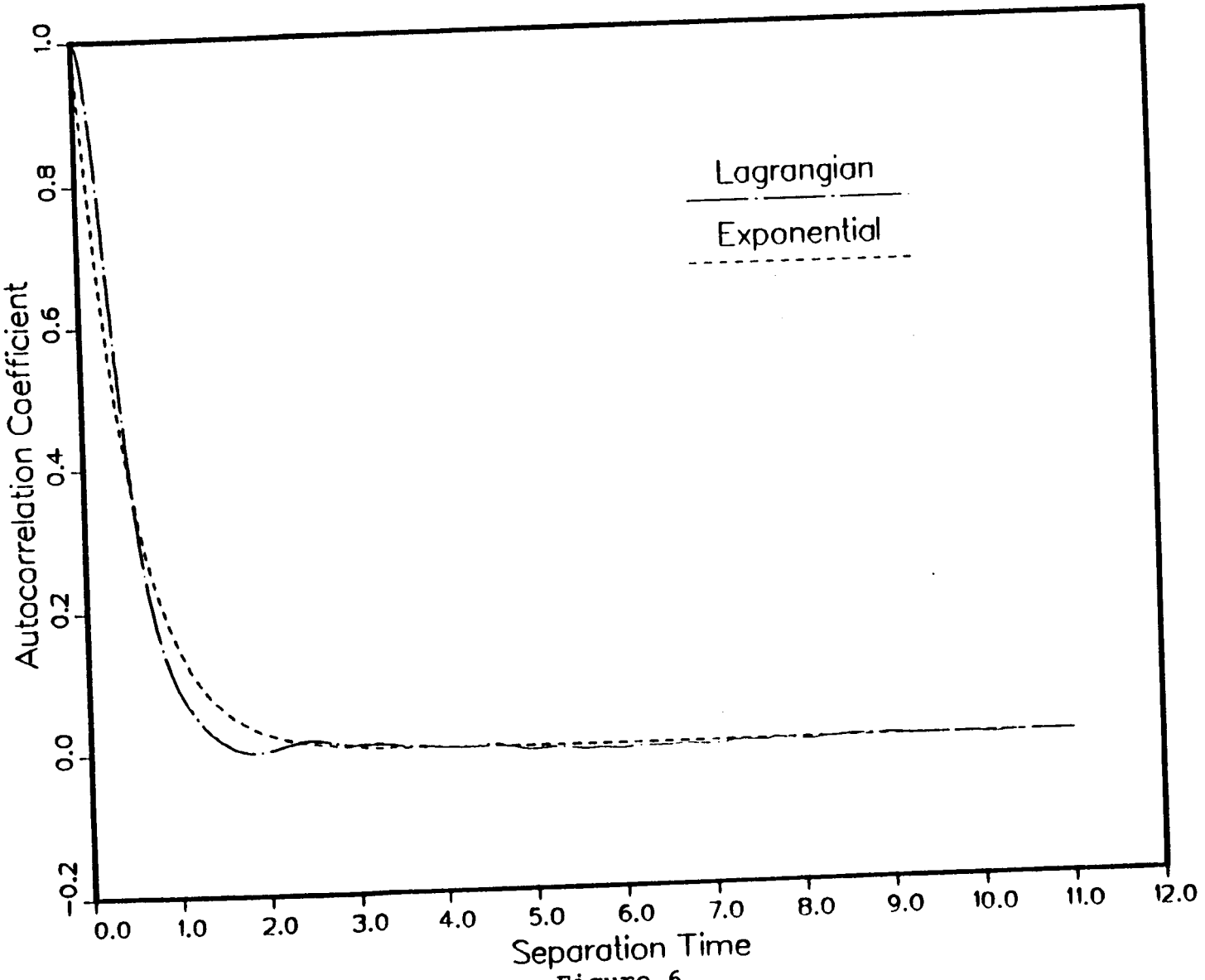

Figure 6

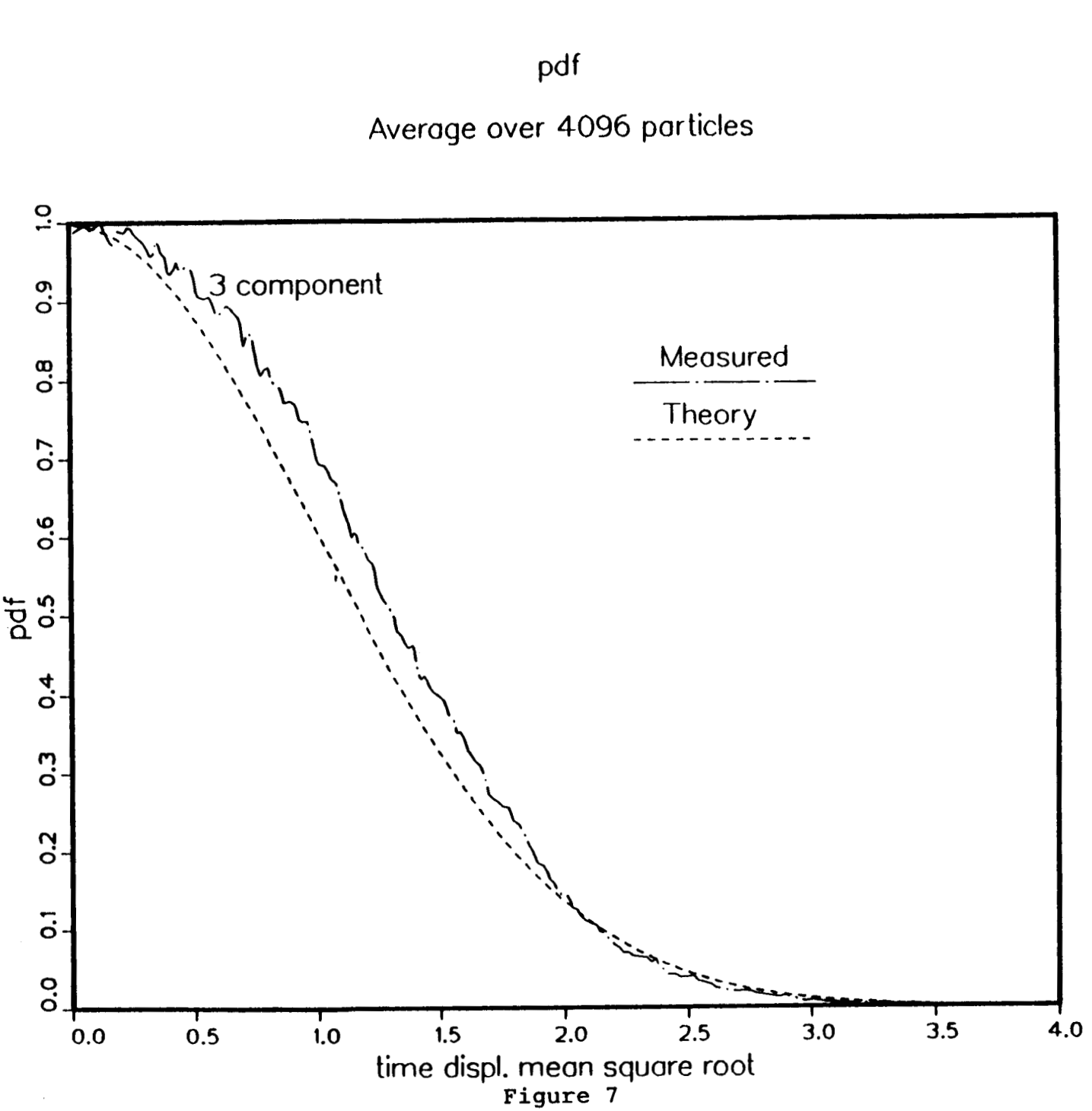

Figure 7

Displacements 2nd order monent

Average over 4096 particles

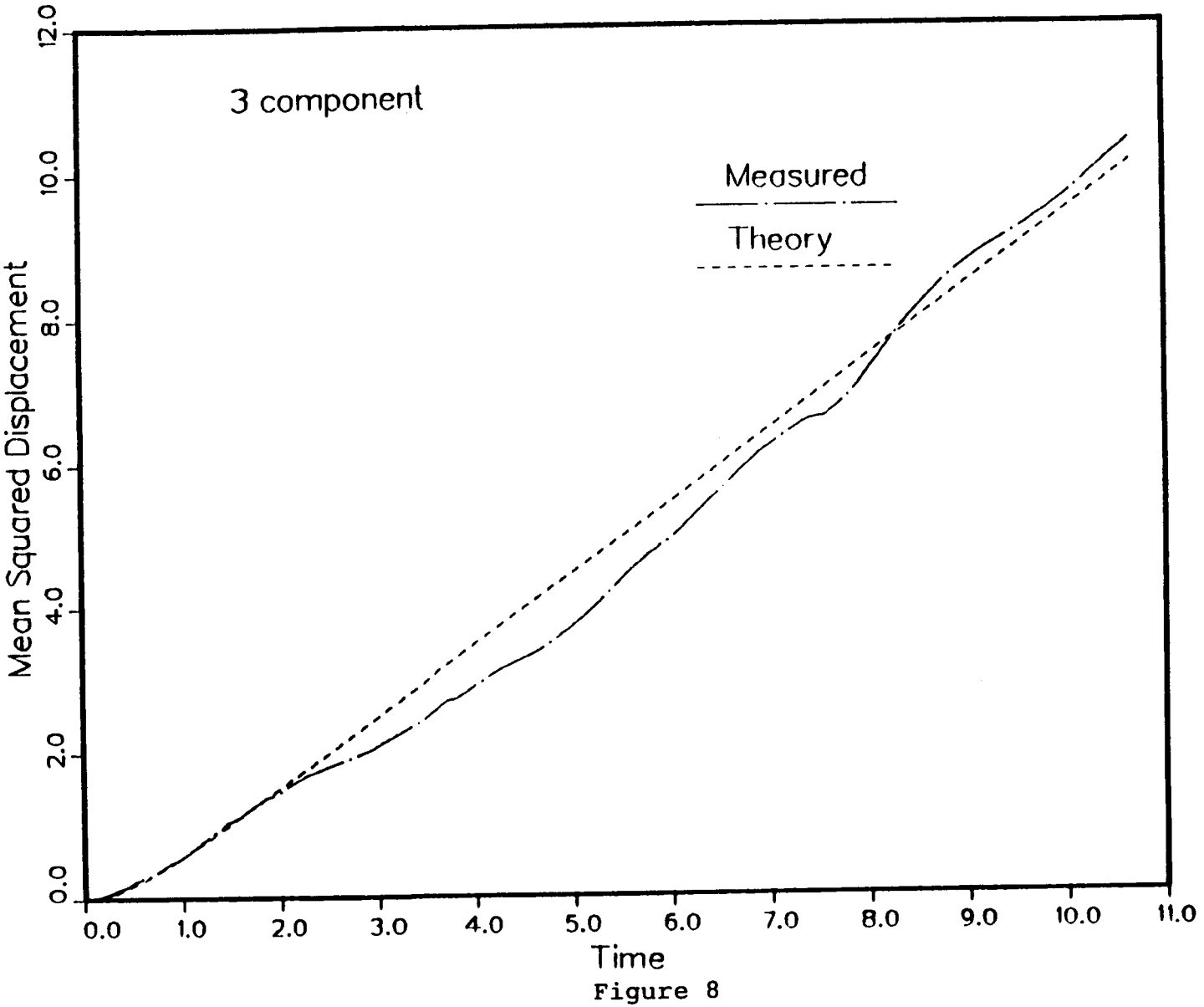

Figure 8

Displacements 2nd order monent DAverage over 4096 particles

Average over 4096 particles

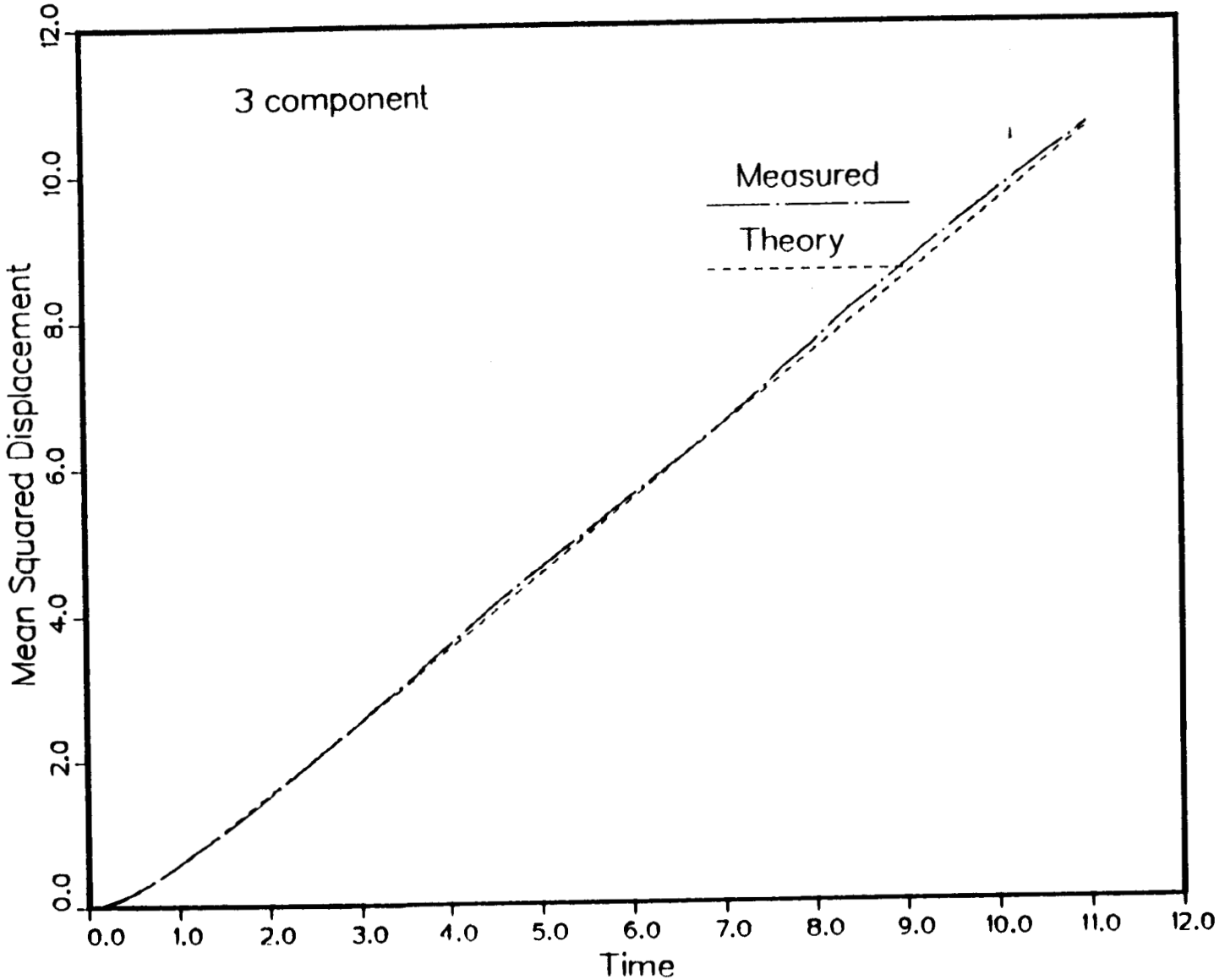

Figure 9

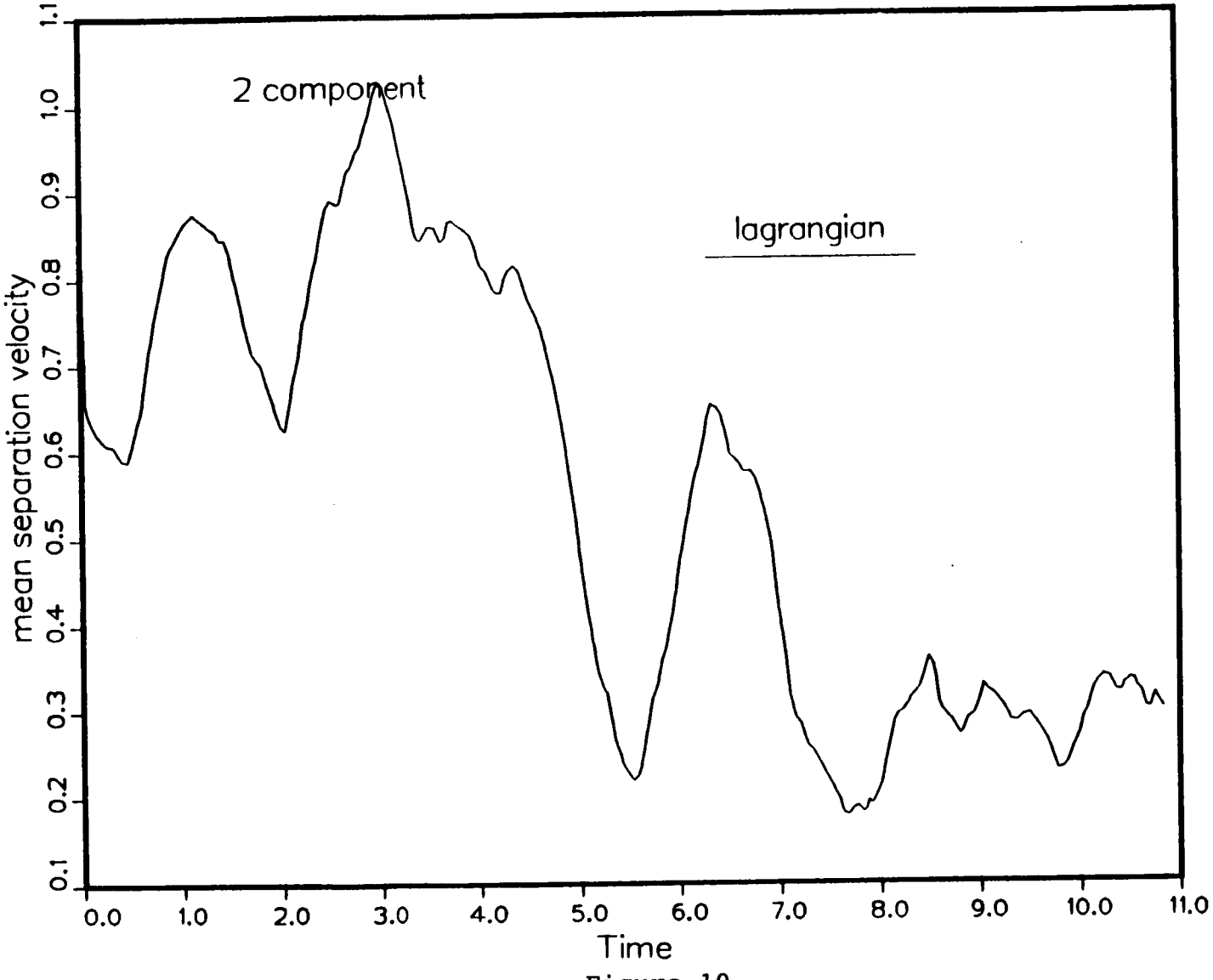

Figure 10

mean separation velocity DD

Average over 4096 particles

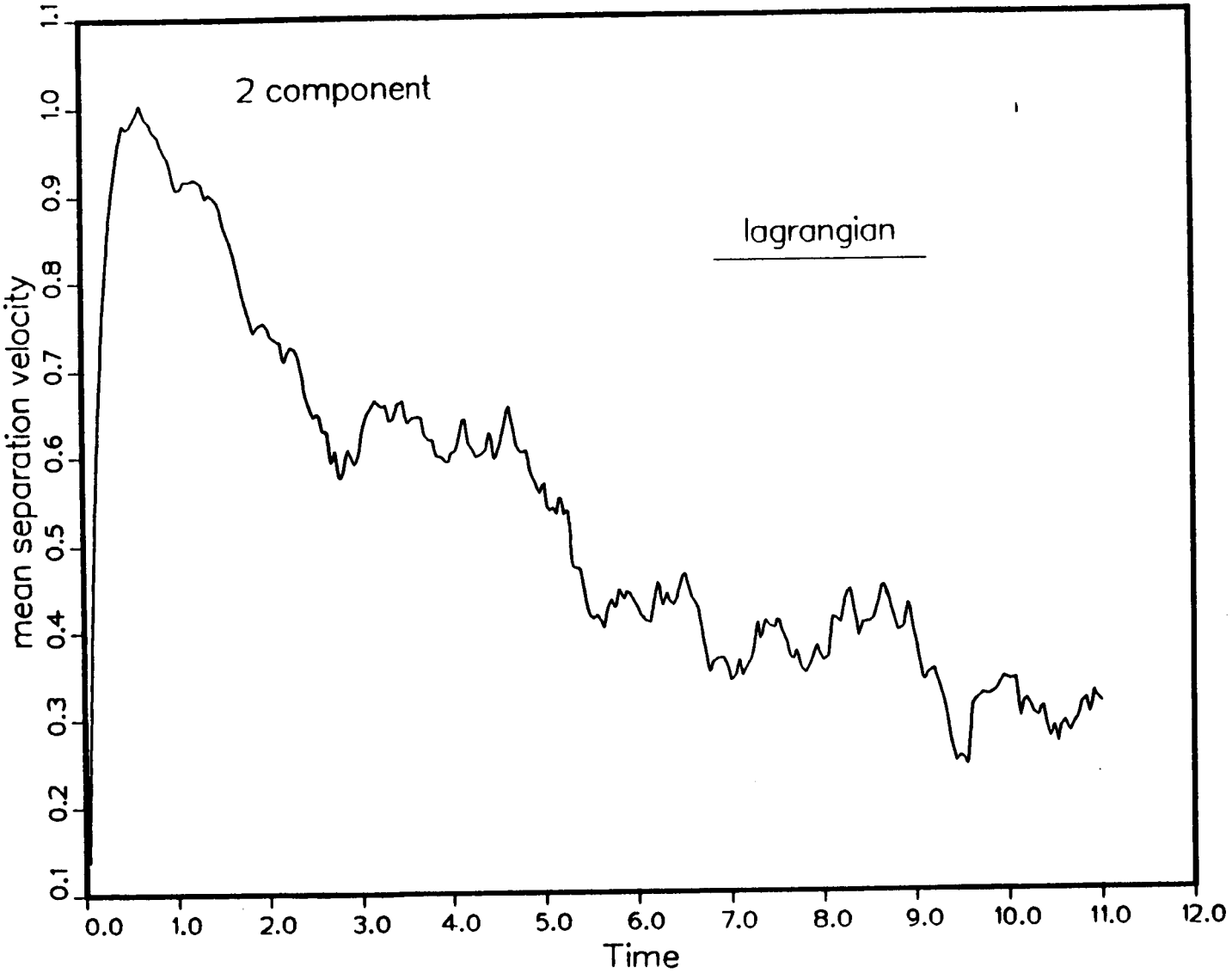

Figure 11

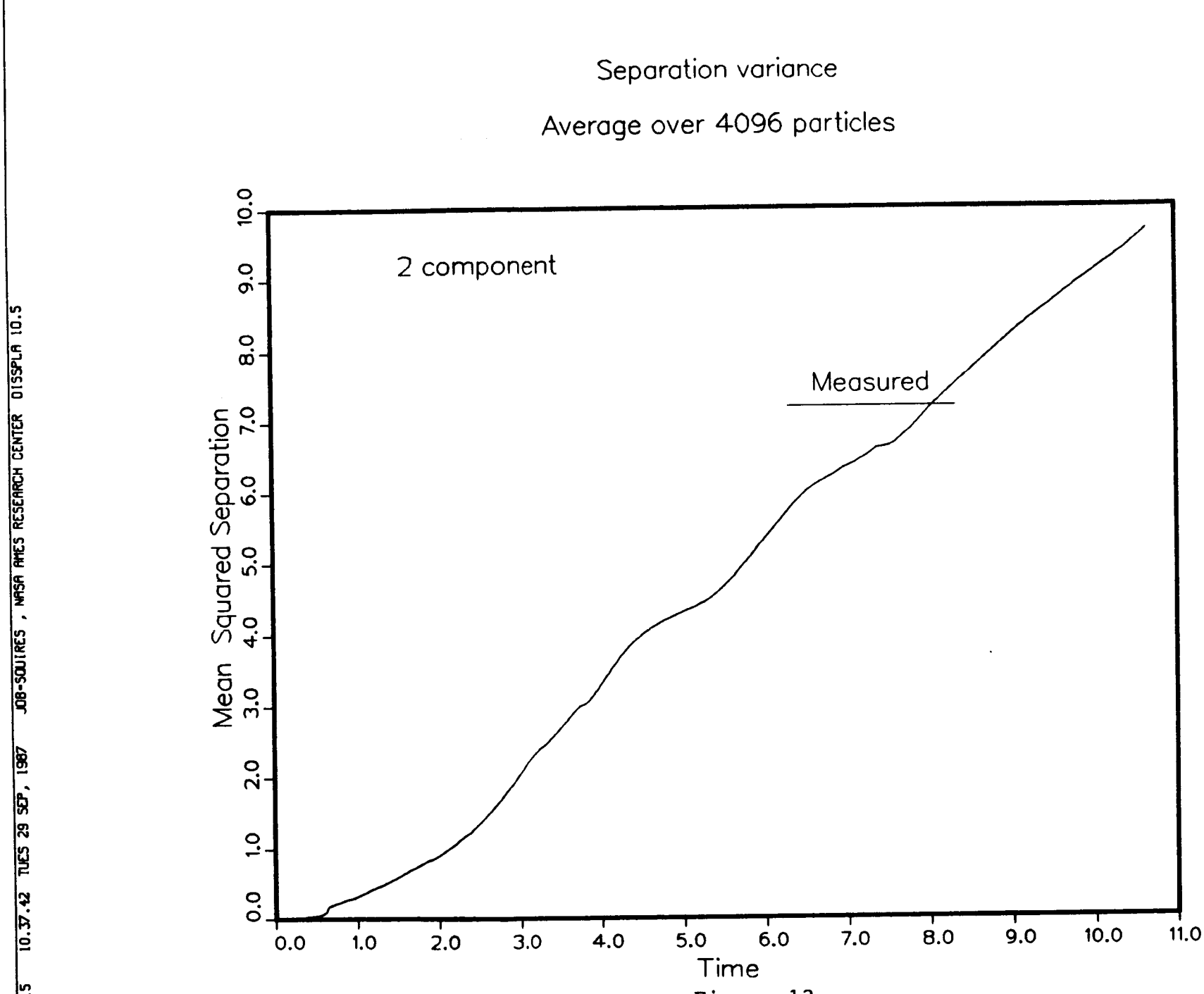
Separation variance
Average over 4096 particles
2 component
Measured
Mean Squared Separation
Time
0.0
1.0
2.0
3.0
4.0
5.0
6.0
7.0
8.0
9.0
10.0
11.0
PLOT 15 10.37.42 TUES 29 SEP, 1987 JOB-SQUIRES , NASA AMES RESEARCH CENTER DISSPLA 10.5

Figure 12

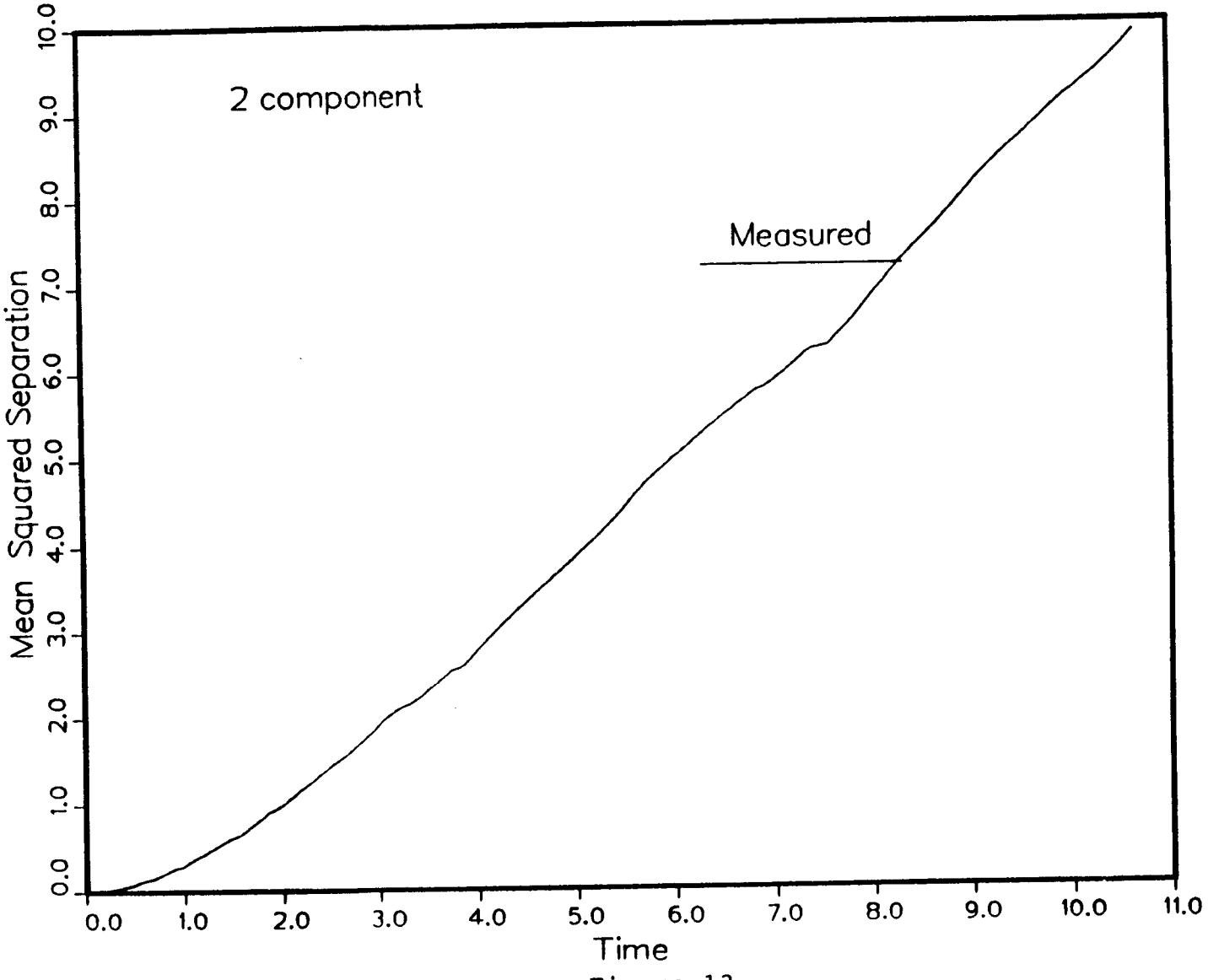

Figure 13

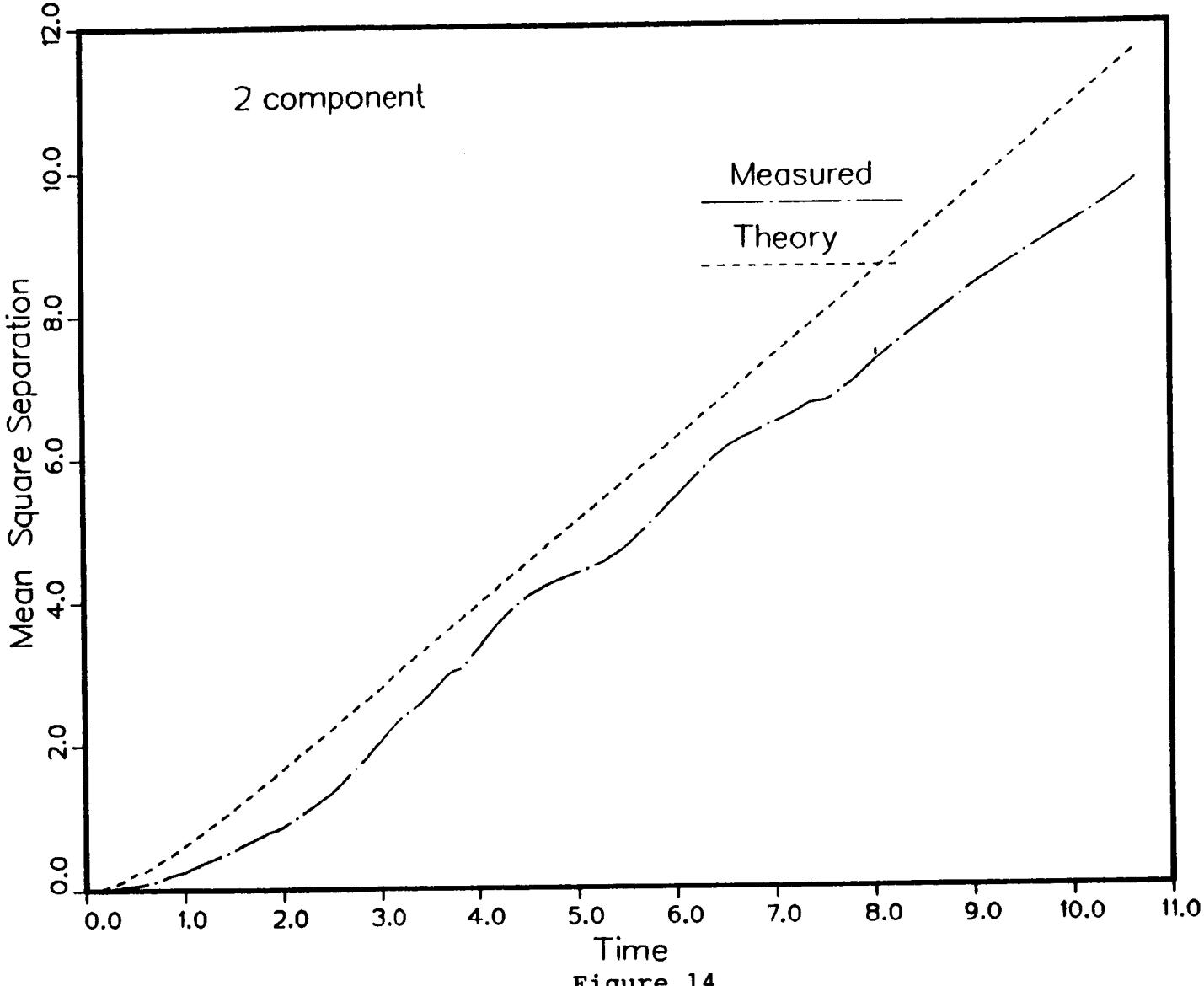

Figure 14

APPENDIX 2

Report by M. Woronowicz and D. Baganoff

Department of AERONAUTICS and ASTRONAUTICS
STANFORD UNIVERSITY

Feasibility Study

Conducted During the Summer Period

1July to 30 September, 1987

on

POSSIBLE USE OF DIRECT PARTICLE SIMULATION

IN THE STUDY OF TURBULENT SHEAR FLOW

Work Supported by the Turbulence Institute
NASA-Ames Research Center
Moffett Field, California 94035

by

Michael Woronowicz - Research Assistant

Donald Baganoff - Faculty Advisor

Department of Aeronautics and Astronautics
Stanford University
Stanford, California 94305

November 22, 1987

OVERVIEW

A feasibility study was conducted during the Summer of 1987 to determine whether particle simulation could be used to study low-speed turbulence in a gas. Additional work was conducted during the Fall of the same year to attempt to resolve several questions that were raised. In trying to determine whether or not turbulence can be modelled in this manner, one must first establish that a suitably large Reynolds number can be reached in the simulation. This requires that we have the means to measure such quantities as kinematic viscosity and Reynolds number based strictly on the behavior of interactions of thousands of particles. This method, which was originally developed by Baganoff for studying hypersonic flows, was adapted to analyze a particular low-speed scenario using an IBM AT microcomputer. Thirty-two thousand particles were used, and computation was restricted to two dimensions.

Stokes' First Problem was considered as a suitable scenario for simulation. In it, a laminar boundary layer develops in both space and time following a similarity scaling law, so the Reynolds number and the shear stress are time-dependent. A program was developed to obtain data on the velocity profile, temperature, and shear stress, and to find a means for computing a Reynolds number. A wide range of freestream velocities were tested ($0.4 < M_\infty < 2.0$). The lower bound on the Mach number was dictated by achieving the highest velocity possible before compressible effects became significant. The importance of this will be explained later. The upper bound was chosen to see what would occur once compressibility became important. Despite the pronounced effects of thermal (random) motion of the particles at low fluid velocities, the simulated velocity profiles fit the theoretical curves nicely. Also, one would expect to find a constant coefficient of kinematic viscosity for incompressible flows, and in this analysis, every simulation gave the same numerical coefficient.

Once the value of the kinematic viscosity was found, the Reynolds number (Re) was computed. Reynolds numbers, based on the boundary layer thickness, of 10 - 400 were obtained in these simulations. (This quantity was computed at different time steps as well as for different freestream velocities.) For a flat plate, a generally accepted, similarly defined Re for the beginning of transition to turbulence is 1220. In a

duct, transition begins at an Re of 2300, based on the diameter of the duct. Also, for Couette flow, Couette measured a critical Re of 1900, based on the distance between the plates (Hinze. Turbulence, second edition, p. 76).

So, it appears that these simulations can achieve the Reynolds numbers associated with the onset of turbulence. Judging from the existing programs on the AT, one can estimate the time requirements needed when running such a program on the CRAY2 computer. While it takes roughly 30 seconds per time step using 32000 particles on the AT, a code adapted to the CRAY2 could use one million particles undergoing time steps every 1.5 seconds. Such a program could easily simulate a three-dimensional flow.

STOKES1

It was decided to simulate a flow that could easily be verified by theory. If such a simulation was successful, one could generate more confidence in the method. An obvious, simple choice was to simulate the flow field of "Stokes' First Problem" (also known as the "Rayleigh Problem"). In the theoretical formulation (see Schlichting. Boundary Layer Theory, seventh edition, pp. 90-91), a semi-infinite fluid, bounded by a stationary wall, is initially at rest. At t = 0+, the wall is suddenly accelerated to a constant velocity of V_w. In time, momentum is transferred to the fluid, and a time-dependent boundary layer develops. For this problem, the analytical solutions for the velocity profile and the shear stress are

$$\frac{v(x,t)}{V_\infty} = \text{erf}(\eta) \qquad \text{where} \quad \eta = \frac{x}{\sqrt{4vt}}$$

$$\tau(x,t) = \tau_w e^{-\eta^2} \qquad \text{where} \quad \tau_w = \rho V_\infty \sqrt{\frac{\nu}{\pi t}}$$

One may define a Reynolds number with a length scale based on the distance

away from the wall where the velocity is 99% of the freestream velocity. The value of the similarity parameter η for which erf (η) = .99 is 1.8214. This gives us a time-dependent Reynolds number of

$$Re_\delta = 3.6\, V_\infty \sqrt{\frac{t}{\nu}}$$

In this program, it was easier to keep the wall stationary and have the fluid, initially having velocity V_∞ everywhere, begin to slow down at the wall. During development of the program, $M_\infty = 0.6$ was used to get the highest fluid velocity possible before compressible effects became significant.

SCATTER

One problem with using particle simulations for low speed flows is due to the fact that fluid motion usually consists of bulk motion of the flow superimposed on the random velocities of the individual particles. In a typical compressible flow, the bulk motion of the flow depends on the Mach number M, where

$$\text{Bulk motion} \quad \alpha \quad M = \frac{u}{a} \qquad \text{where} \quad a^2 = \gamma RT$$

$$\text{Thermal motion} \quad \alpha \quad T \quad \alpha \quad \overline{C^2} \qquad \text{where} \quad \overline{C^2} = 3RT$$

So, $a \sim C_{rms}$. Hence, as M increases, $u / a \sim u / C_{rms}$ increases, and thermal fluctuations become a smaller fraction of the total velocity. Also, since

$$\text{dispersion} = \frac{\sigma}{\bar{x}} = \frac{1}{\sqrt{N}}$$

where N = number of particles (normal distribution)

there is less statistical scatter with more particles in the region of interest and particle density increases.

STOKES1 RESULTS

In solving Stokes First Problem, one finds that the governing differential equation scales according to a similarity parameter $x/\sqrt{4vt}$. Because of this scaling, it was decided to save data of a particular simulation at time steps that were related to each other by a certain constant factor. Usually, data was saved for time steps from 32 to 2048 that were related to each other by factors of two.

The size of the computational box was 20 divisions high along the wall and 80 divisions long normal to it. These divisions were used for calculating averaged values of physical quantities from the particle populations lying within each division. Thirty-two thousand particles were used in this two-dimensional system, because this number made good use of the allowable array lengths available with the large memory model on the AT. (Using the huge memory module would increase run times significantly.) As in the theoretical formulation, only the development of quantities normal to the wall were calculated. When data was to be obtained during a certain time step, the number of particles in each of the 80 columns was totaled, as well as the sums of each particles' three velocity components, their squares, and sums of x-velocity times y-velocity. Further, in computing velocity, density, temperature, pressure, and shear stress profiles normal to the wall, another averaging took place. In calculating a quantity, at each x position, corresponding to one column, the values of the two adjacent columns were added to it. The resulting value was then divided by the number density of those three columns. This data sampling occurred at a point in the program after the particles' positions had been updated but before the collision algorithm had been applied in order to get values before equilibrium occurred through collisions.

Later, data from a run, which consisted of sets of data from various time steps,

were called up, and velocity profiles were plotted. If these profiles were to follow the theoretical similarity scaling law, one could fix the time at an arbitrary value and vary the normal distance. Then, the profiles would collapse onto each other. It can be seen from the included figures that the data collapses on the similarity parameter very well. Figure 1 shows the similarity profile for M_∞= 0.6 scaled to fit a time step t of 32. Figures 2 and 3 show the same similarity profile scaled to t = 512 and 2048, respectively.

At this point, we may either pick a Reynolds number and then obtain a coefficient of kinematic viscosity, or we may find the kinematic viscosity and from that find the Reynolds number. The latter method was chosen, because one can easily fit the theoretical velocity profile to the scaled data and get a kinematic viscosity coefficient from the best-fitting similarity parameter. As expected, this coefficient remains constant regardless of the time step used to scale the data. Also, since the temperature profile is roughly constant (see figure 4), this coefficient remains constant over the entire range of Mach numbers tested. The best-fitting similarity parameter yielded a kinematic viscosity coefficient of .0562 squared divisions per time step. Because no mean free path was introduced in this model, this coefficient is not dependent on the density of particles in the system. After finding this coefficient, the Reynolds number Re and the wall frictional coefficient $C_{f,w}$ were calculated. For the ranges of time steps and freestream velocities tested, Re ranged from 10.3 to 413 and $C_{f,w}$ ranged from 0.00985 to 0.394.

Once these quantities were found, the calculated dimensionless temperature and density profiles normal to the wall were plotted in order to determine whether or not incompressible assumptions were being violated.

Then, the Mach number was increased to supersonic speeds. This was done in order to observe the effects of compressibility on the model and perhaps find a limit beyond which the velocity would no longer scale with the similarity parameter. Instead, it was discovered during this study that, although the temperature profile normal to the wall stays fairly constant at lower speeds, at higher speeds it builds up near the wall, and this build-up apparently scales with the same similarity parameter as the velocity!

Notice how the temperature data changes as the Mach number increases from 0.6 to 2.0 at a fixed time scale of 2048 timesteps (figures 4 - 6). The temperature of the wall (T_w) was constrained to be the same as that of the initial, undisturbed fluid; but as the Mach number increases, there is increased collisional activity of the particles near the wall, so in that region, T increases. The result is the "bulge" in T which can clearly be seen in the supersonic data. Figures 6 through 8 show that for time step scales of 32 through 2048, this bulge apparently scales with the similarity parameter $x/\sqrt{4vt}$ for fixed Mach number ($M_\infty = 2.0$). Also, notice how the density profile in these figures changes with distance. As one might expect, the density for an ideal gas at constant pressure is lowest in the region where the temperature is highest.

Finally, the theoretical dimensionless shear stress profile was compared to the shear stress data, as shown in figure 9. Although the function seems to fall within the scatter of the data points, there is too much scatter to tell how well it represents the data. We found this to be rather disappointing. At this time, it is not understood why there is so much variance in these data points. Attempts to resolve this question caused this report to be delayed.

COMPUTATIONAL TIMES

Computation on the AT took thirty seconds of user time per time step for 32000 particles. Based on estimates done by Jeff McDonald when he adapted a similar code for the CRAY2 from the AT, running a modified version of this program on the CRAY2 computer would achieve the same results for 10^6 particles in approximately 1.5 seconds per time step. In order to do this, one would have to make use of vectorization on the CRAY2. This would allow about 2400 time steps per hour for a flow represented by over 31 times more particles than in this study. Moreover, such a flow could be three-dimensional.

There is a tradeoff involved, however. If one wanted to re-create the model

studied this summer, one could take advantage of the fact that the dispersion, or statistical scatter, could be significantly decreased by using more particles in a two-dimensional box of identical dimensions. If 10^6 particles were used, the particle density would be over 30 times as great, and the dispersion would be over five times smaller. Alternately, one could keep the same particle density, roughly, and give the system a third dimension. For 10^6 particles, that third dimension would have 31 divisions in length. So, a three-dimensional simulation has an accuracy disadvantage compared to its two-dimensional counterpart for a fixed number of particles. The resolution of this compromise would depend on the goal of the investigator.

FREE SHEAR

Also, a two-dimensional free shear flow was constructed, where two parallel particle streams of equal width, having the same velocity but travelling in opposite directions, were allowed to interact at some initial time. The simulation was displayed on a color monitor with one particle stream in red and the other in blue. As the system evolved in time, mixing of the streams was observed, with diffusional length growing with time. The overall velocity profiles, temperature T, and shear stress τ_{xy}, were computed from suitably averaged moments of velocity across the entire width of the system. As the speeds and particle densities were increased, there was less statistical scatter due to thermal motion and better visualization of the flow. Even though mixing was evident, the diffusional length grew with a square root dependence on time, just as it did in the Stokes First Problem model. This indicates that the mixing was laminar over the period observed (roughly 1000 time steps), which may not be surprising since this setup was not unlike that for Stokes First Problem. The difference with this setup was that the wall had been replaced by the boundary of a gas travelling in the opposite direction.

At this time it is not clear whether or not such a flow would remain laminar or at some later time become turbulent. The length of time needed to observe significantly higher Reynolds numbers was prohibited by the time taken to run the program on the AT.

CONCLUSIONS

So, it appears that particle simulation can model simple, low-speed, gaseous flows, and that useful physical quantities can be extracted from them. Unfortunately, at this time, the shear stress data has too much scatter in it to tell how well it is being predicted. In doing this exploratory study, the code was kept as simple as possible to get results quickly. Perhaps something important yet subtle has been omitted from the computation. Further work is being directed toward studying the shear stress. Also, it may be necessary to introduce a variable mean free path so that flow parameters such as the kinematic viscosity may be varied. An enhanced capacity to vary these parameters would increase the utility of this model to simulate different flows.

At this time, it is not clear whether or not a particle simulation would be suitable for modelling turbulent flows. This would depend on the results obtained by making the changes discussed above. With a capability to increase Reynolds numbers efficiently, either through the use of a more powerful computer, or by an enhanced capability to vary the flow parameters, one could then simulate a flow which should become turbulent, resulting in a dramatic change in velocity and velocity moment profiles, and observe whether or not the particle model would exhibit such a transition. Such a test would better determine the suitability of this method for studying turbulence.

ORIGINAL PAGE IS
OF POOR QUALITY

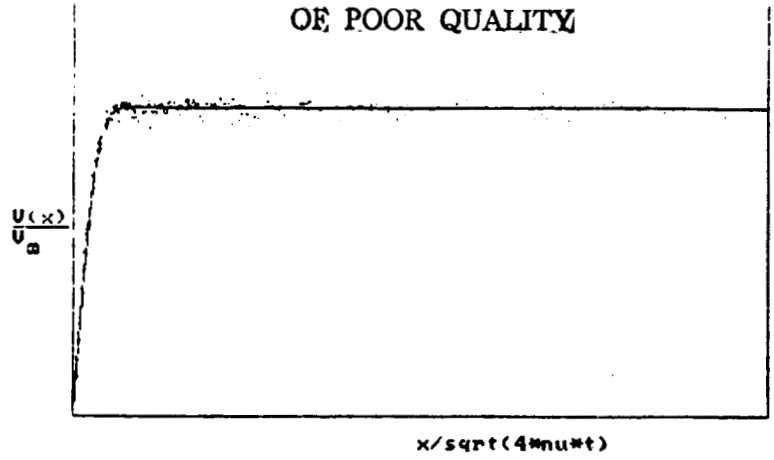

Select data_set no.
/floppy/V3o5.32.stks1
/floppy/V3o5.64.stks1
/floppy/V3o5.128.stks1
/floppy/V3o5.256.stks1
/floppy/V3o5.512.stks1
/floppy/V3o5.1024.stks1
/floppy/V3o5.2048.stks1

Time scaled to t = 32
Select 'sim. var. denom.'
4 * nu * t = 7.19
nu = 0.0562
M_∞ = 0.6000
U_∞ = 0.1800

Reynolds no. = 15.50
C_f = 0.262598

Figure 1

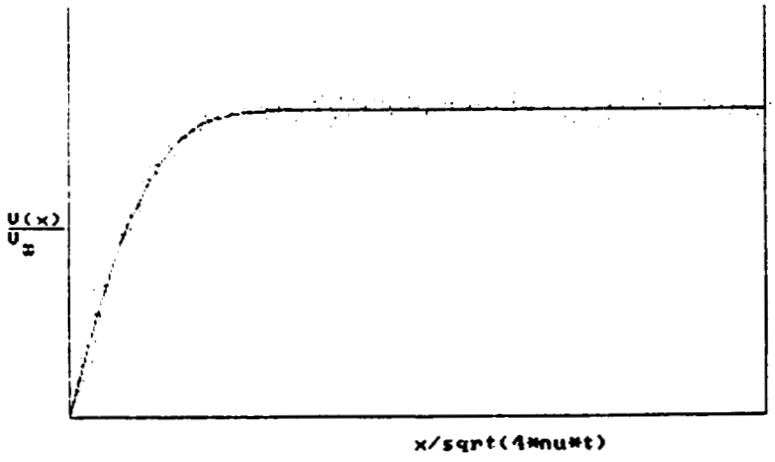

Select data_set no.
/floppy/V3o5.32.stks1
/floppy/V3o5.64.stks1
/floppy/V3o5.128.stks1
/floppy/V3o5.256.stks1
/floppy/V3o5.512.stks1
/floppy/V3o5.1024.stks1
/floppy/V3o5.2048.stks1

Time scaled to t = 512
Select 'sim. var. denom.'
4 * nu * t = 115.00
nu = 0.0562
M_∞ = 0.6000
U_∞ = 0.1800

Reynolds no. = 61.99
C_f = 0.065650

Figure 2

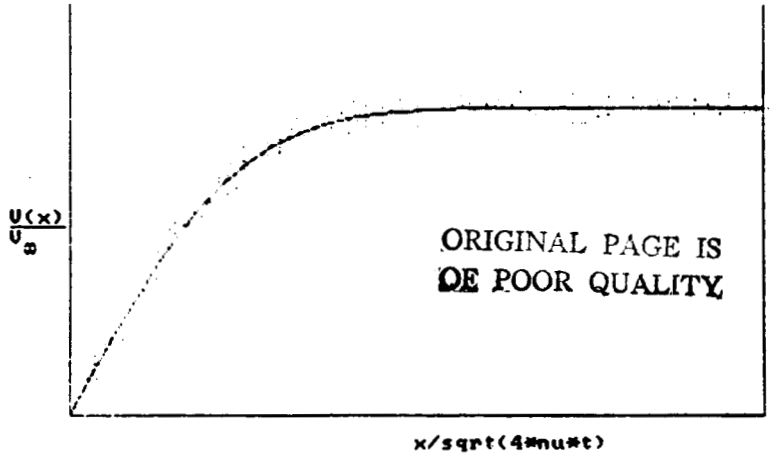

Select data_set no.
/floppy/V3o5.32.stks1
/floppy/V3o5.64.stks1
/floppy/V3o5.128.stks1
/floppy/V3o5.256.stks1
/floppy/V3o5.512.stks1
/floppy/V3o5.1024.stks1
/floppy/V3o5.2048.stks1

Time scaled to t = 2048
Select 'sim. var. denom.'
4 * nu * t = 460.00
nu = 0.0562
M_∞ = 0.6000
U_∞ = 0.1800

Reynolds no. = 123.97
C_f = 0.032825

Figure 3

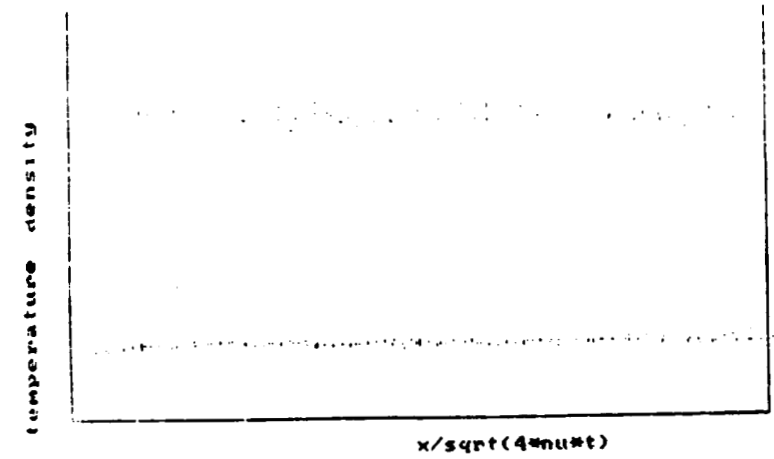

Select data_set no.
/floppy/V3o5.32.stks1
/floppy/V3o5.64.stks1
/floppy/V3o5.128.stks1
/floppy/V3o5.256.stks1
/floppy/V3o5.512.stks1
/floppy/V3o5.1024.stks1
/floppy/V3o5.2048.stks1

Time scaled to t = 2048
M_∞ = 0.6000

Figure 4

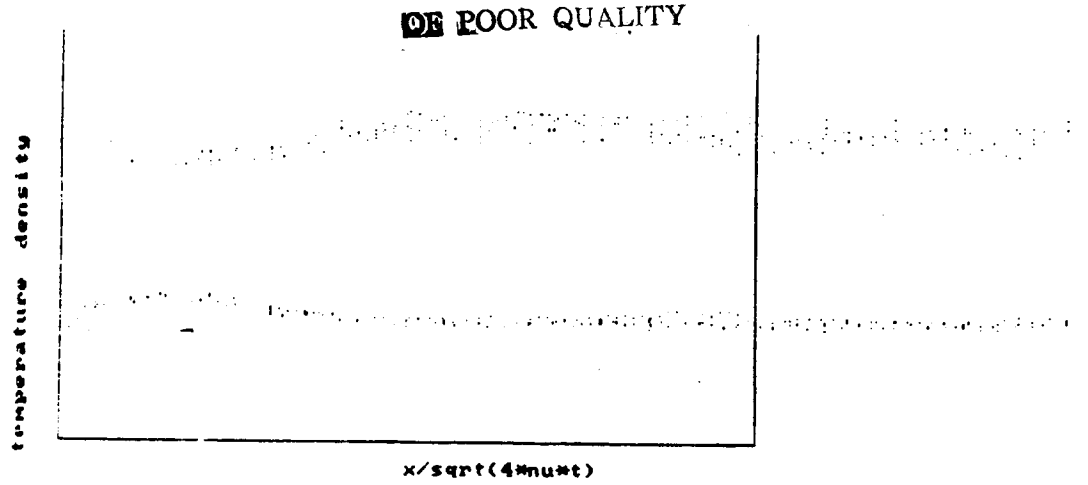

Select data_set no.
/floppy/V3o2.32.stks1
/floppy/V3o2.64.stks1
/floppy/V3o2.128.stks1
/floppy/V3o2.256.stks1
/floppy/V3o2.512.stks1
/floppy/V3o2.1024.stks1
/floppy/V3o2.2048.stks1

Time scaled to t = 2048
M_∞ = 1.5000

Figure 5

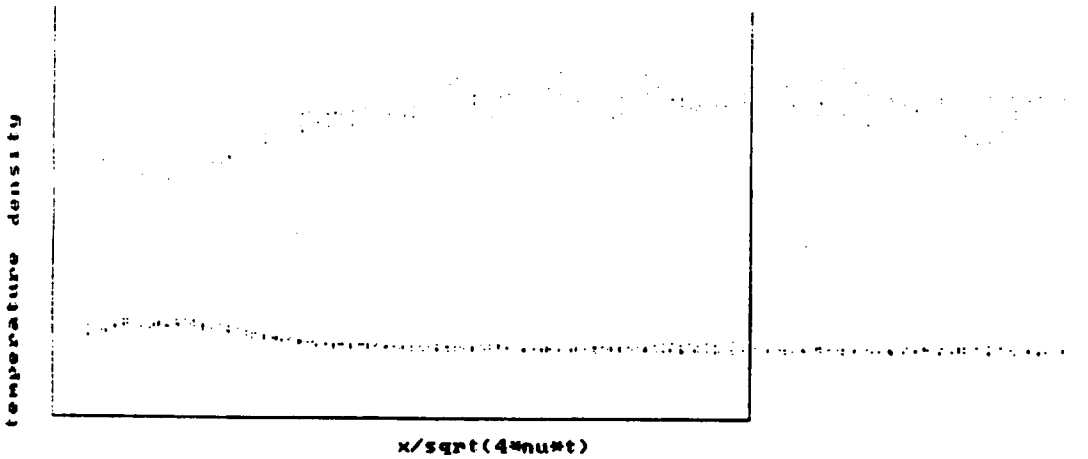

Select data_set no.
/floppy/Vtwo32.stks1
/floppy/Vtwo64.stks1
/floppy/Vtwo128.stks1
/floppy/Vtwo256.stks1
/floppy/Vtwo512.stks1
/floppy/Vtwo1024.stks1
/floppy/Vtwo2048.stks1

Time scaled to t = 2048
M_∞ = 2.0000

Figure 6

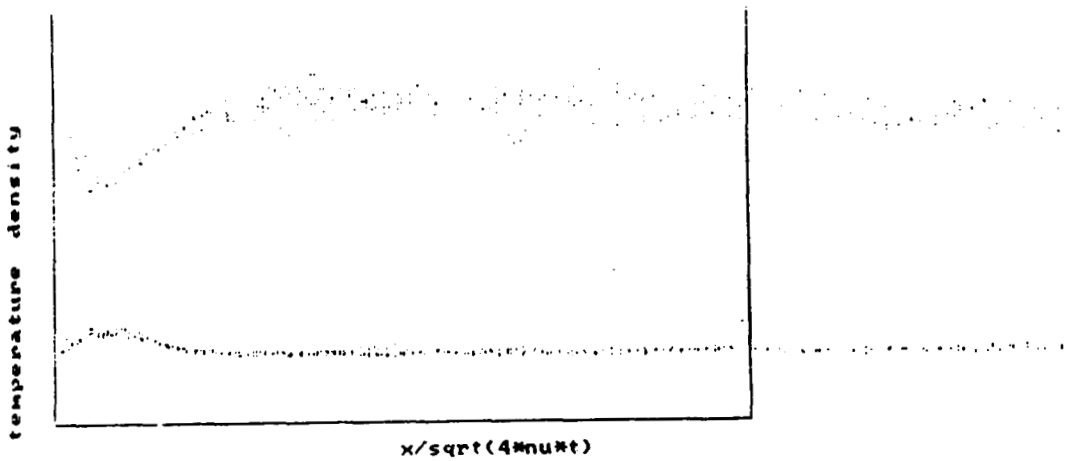

Select data_set no.
/floppy/Vtwo32.stks1
/floppy/Vtwo64.stks1
/floppy/Vtwo128.stks1
/floppy/Vtwo256.stks1
/floppy/Vtwo512.stks1
/floppy/Vtwo1024.stks1
/floppy/Vtwo2048.stks1

Time scaled to t = 512
M_∞ = 2.0000

Figure 7

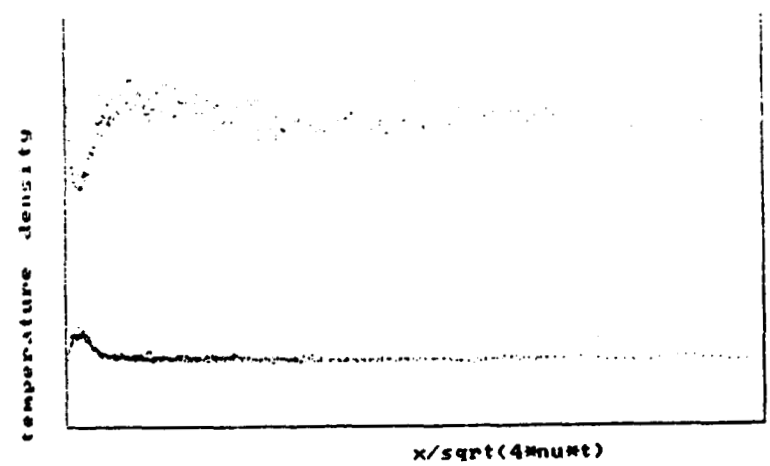

Select data_set no.
/floppy/Vtwo32.stks1
/floppy/Vtwo64.stks1
/floppy/Vtwo128.stks1
/floppy/Vtwo256.stks1
/floppy/Vtwo512.stks1
/floppy/Vtwo1024.stks1
/floppy/Vtwo2048.stks1

Time scaled to t = 32
M_∞ = 2.0000

Figure 8

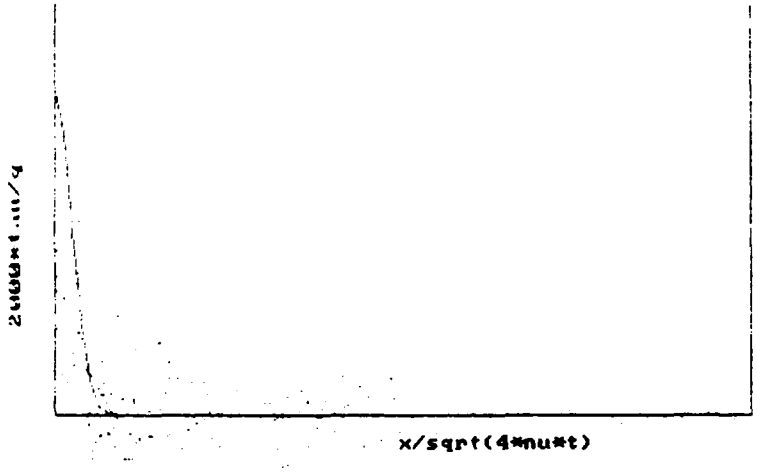

Select data_set no.
/floppy/Vtwo32.stks1
/floppy/Vtwo64.stks1
/floppy/Vtwo128.stks1
/floppy/Vtwo256.stks1
/floppy/Vtwo512.stks1
/floppy/Vtwo1024.stks1
/floppy/Vtwo2048.stks1

Time scaled to t = 32
M_∞ = 2.0000

Figure 9

APPENDIX 3

Report by T. R. Osborn and H. Yamazaki

Study of the Motion of Particles With a Random Walk in an Isotropic Turbulent Field

Hidekatsu Yamazaki
Thomas R. Osborn
Chesapeake Bay Institute
The Johns Hopkins University

1. Introduction

This report discusses some of the preliminary results obtained from our visit to Stanford Univ. during Oct.-Nov. 1987. The major objective of our research is to study encounter rates between planktonic particles in a turbulent fluid. The results of this study can be applied to the food web of oceanic plankton. The typical size and the motion of a single step of a zooplankter are comparable to the Kolomogorv scales for oceanic turbulence (where the rates of dissipation are $10^{-1} \sim 10^{-6}$ cm^2/sec^3). Therefore we expect to observe some effects on planktonic motion induced by a turbulent field, and this has an influence on the contact rates between pray and predator. Although the intuitive argument is simple, the theoretical study is extremely complicated because of the spatial and temporal correlation of the turbulence field.

Direct simulation of Navier-Stokes equation enables us to combine the effects of a turbulent velocity field with a random walk used to model planktonic motion relative to the water. We made use of pseudo-spectral code for turbulent simulations developed by NASA and the Stanford University group. An isotropic turbulent field was generated on 64^3 grid points using a forcing scheme. The forced simulation is desirable because we can study the variation in contact rate at a constant turbulent intensity. The velocity calculation started from a field that had reached a steady state. The kinematic viscosity was 0.1. The simulation showed that the Reynolds number was 20 and the rate of dissipation was 202. The time step interval was 0.00046. We incorporated eight different sizes of random walks, in groups of 512 particles. The standard deviations of the random walks were the following,

1) 0, namely no random walk,
2) v_η
3) $5v_\eta$
4) $10v_\eta$
5) $25v_\eta$
6) $50v_\eta$
7) $100v_\eta$
8) $500v_\eta$

where v_η is Kolomogorv velocity scale $(\epsilon\nu)^{1/4}$ for a given rate of dissipation ϵ and kinematic viscosity ν. Before we pursued our major objective we examined the statistics of velocity vectors for each particle and the statistics of nearest neighbor distances.

2. Particle contact rates

We traced the eight groups of particles over 1200 steps (these calculation were a modification of K. Squires program, without whose help we could not have done this work in such a short time). The first 600 steps and last 600 steps were computed separately. We used the first 600 steps for the purpose of preliminary evaluation of contact rates between particles. Since we are interested in a difference in the contact rate with and without a turbulent field, we also simulated the motion of particles by a pure random walk with no turbulence. The particles were released from randomly distributed locations (by a uniform distribution) inside

the simulation domain (box).

The calculation of contact was done in a second program after the program that moved the particles about. Particles that exited the box under consideration were moved back in through the opposite face so that the densities of predator or prey were not changed by particles escaping. When the distance between two particle becomes less than a threshold, the particles are considered to be in contact. We treated two cases for the prey particle after the contact. In the "without replacement" case, the particle (prey) was removed from the box. For the "with replacement" case, we would keep the particle "hidden" for a certain interval and then put it back into the system. The hiding of the particle was to avoid artificially large contact rates due to repeated contact between the same two particles. We present the result from the "without replacement" case in this report. It was found that the "with replacement" case had a source code problem and a corrected calculation is required. The with replacement calculation is the desirable result as it is the easiest to interpret.

Since we have eight groups of particles many combinations of "prey-predator" conditions are possible. We calculated 28 cases of "prey-predator" contacts (Table 2.1). Predators with a large random walks contact all of prey before the 600th time step, so it is necessary to normalize the number of contacts. Let n be the number of prey contacted, n is less than 512 for the small random walks, and N the total number of predators (512). The time step t, when the last prey contacted, can be used to average the time interval of searching for a prey. The normalized contact rates γ is defined as follows,

$$\gamma = nT/(Nt)$$

where T is the total time steps (600). The upper values of each cell is without turbulence and the lower value is with turbulence. The 6 cases for the smallest random walks reveal the result we expect, that turbulence should increase the contact rates between prey and predator. The rest of the values indicate that the turbulence field is an insignificant factor for the contact rates. While we are pleased with the preliminary result, it still needs to be put into a biological context (scaled with ϵ and ν) and then related to the analytical results in Rothschild and Osborn (attached and in press in the Journal of Plankton Research)

Future work

It is apparent that our results while encouraging are still primitive. There are both short term and long term aspects to the problem. In the short term we need to modify and correct our computer code that does the contact calculations. Some of this has been done already. We can then fully analyze the calculations from the 64^3 model that were performed and saved this last fall. Those result can then be rationalized with the analytical calculations and form the basis for a first paper on the approach and the results.

In the longer term, we need to perform some calculations at higher Reynolds number presumably on a 128^3 grid. The planktonic motion needs to be expanded from a simple random walk to a series of flights that last over several time steps of the calculation. This change will increase the amount of calculation because another time scale is introduced (length of flight of the predator along the same path). As well, it will become important to incorporate behavioral responses to ingestion in the model. After eating, or when well fed, the predators do not hunt as hard; when starving, searching for food and the ability to escape predators is reduced.

Essentially the short term projects are improvements of the technique and verification of the results. The long term projects are expanded development and utilization of the numerical calculation for studying the interaction of biological system with the turbulent fluid.

Table 1 Contact rates between particles. The heading in each column and row refers to the random walk group. The upper number in each pair of data values is without random walk and the lower number is for random walk plus the turbulence.

prey\predator	2	3	4	5	6	7	8
1	0.09	0.17	0.33	0.77	0.98	1.39	5.08
	0.25	0.34	0.46	0.78	0.99	2.23	6.67
2	X	0.16	0.32	0.73	0.99	2.21	6.12
	X	0.31	0.47	0.79	0.99	1.57	5.22
3	X	X	0.32	0.76	0.98	1.44	5.88
	X	X	0.46	0.78	0.98	2.46	6.74
4	X	X	X	0.76	0.98	1.73	6.32
	X	X	X	0.79	0.98	1.83	5.45
5	X	X	X	X	0.99	2.13	4.48
	X	X	X	X	0.99	1.97	8.11
6	X	X	X	X	X	2.33	4.29
	X	X	X	X	X	2.05	5.41
7	X	X	X	X	X	X	5.17
	X	X	X	X	X	X	5.61

3. Statistics of particles

3.1 Velocity vectors of particles

Velocity components generated from the turbulent simulation for each particle compose a set of time series. A velocity component at a particular time step correlates with the previous time step. Following the conventional notion of Lagrangian auto-correlation, the velocity correlation decreases exponentially as the time lag increases. Since we add a random walk to the particle motion at each time step, the conventional arguments are no longer valid. We examined the averages of the velocity time series of each particle. As the size of the random walk becomes larger, at each time step the particle is forced away from a position where the particle would be located by the turbulent field and the time series of velocity becomes uncorrelated with its own past. Therefore we expect the average values of the velocity components for large random walk should follow the distribution of the mean from white noise. On the other hand the average velocity components with no random walk must follow the distribution law of a correlated random variable. Let u_{ij}, v_{ij} and w_{ij} be velocity components of i-th particle at j-th time step. These values comprise the velocity vector **a** and the magnitude of **a** is

$$a^2_{ij} = u^2_{ij} + v^2_{ij} + w^2_{ij}.$$

We examined the averages of velocity components u,v,w and velocity vector **a** over 200 time steps, namely the following values were calculated

$$U_i = \Sigma\, u_{ij} / N$$
$$V_i = \Sigma\, v_{ij} / N$$
$$W_i = \Sigma\, w_{ij} / N$$
and
$$A_i = \Sigma\, a_{ij} / N.$$

Table 3.1-3.4 show the statistics of each average value. Since the random walk forces a particle to move in an uncorrelated fashion, the particle with the large steps tends to lose correlation from one time step to the next. The mean of U, V and W approach zero for larger random walks and the range of the statistics becomes smaller. A random sampling from the turbulence field, so that each time series of u, v and w were uncorrelated, showed a good agreement with case 8). Some of particles without random walk are trapped in eddies and some are scattered around. Therefore the averages of U, V and W showed the large standard deviation for a short realization period in the present case (200 steps). A careful inspection of the standard deviation indicates some peculiar interaction of turbulence field with random walk for cases 2) and 3). All of the statistics are monotonici with increasing random walk step size except these two cases.

The random walk was generated from a normal distribution for all of our simulations. To ensure that no programing errors existed in the codes, a random walk based on the uniform distribution (from the Cray intrinsic function) was also applied to each step and the result showed the same tendency as the normal distribution.

Table 3.1 Statistics for U_i

	mean	s.d	min	max
1)	-0.2405701	4.4174653	-11.1525369	11.2729212
2)	0.1061830	4.6179897	-12.4469889	10.8448361
3)	-0.1063024	4.4741023	-12.7496693	10.6039775
4)	0.1637198	4.3686518	-10.7305665	10.0886646
5)	0.0739651	3.9530263	-10.3270934	11.1192905
6)	-0.0484558	3.0176252	-9.6488662	8.6306654
7)	0.0049584	1.9290495	-6.3919247	5.7244361
8)	-0.0057150	0.4719053	-1.4193553	1.2998666

Table 3.2 Statistics for V_i

	mean	s.d	min	max
1)	-0.5182599	4.1638463	-12.6059994	11.6511822
2)	-0.2592903	5.0128338	-14.2338938	11.9635239
3)	0.5663336	4.6510084	-10.7875769	12.6121930
4)	0.7882887	4.5643164	-9.9557783	14.6300351
5)	-0.0366833	4.1046428	-9.7325182	10.4931608
6)	0.1122861	2.9682378	-9.5482282	8.0167097
7)	0.0345716	1.9081249	-6.4678161	7.8802499
8)	-0.0079068	0.4806509	-1.8767631	1.5038711

Table 3.3 Statistics for W_i

	mean	s.d	min	max
1)	-0.8477828	4.7996655	-11.5839232	12.2917635
2)	-0.1974391	4.6724461	-14.8436250	10.1079898
3)	-0.4030535	4.9459295	-12.9826462	12.6153774
4)	-0.1622836	4.7454426	-14.2204286	12.1482159
5)	0.7569673	4.2470180	-13.7572350	9.3310843
6)	0.7373272	3.0956171	-8.6091972	9.6507205
7)	0.0727480	1.8895971	-6.1635830	6.2546522
8)	-0.0084084	0.5023862	-1.5490949	1.4636020

Table 3.4 Statistics for A_i

	mean	s.d	min	max
1)	7.8896638	2.8654964	0.9208719	14.9406667
2)	8.5395250	2.9846524	1.4578940	16.9043228
3)	8.5713267	2.7004234	2.3444629	15.5812644
4)	8.3468284	2.8001345	1.2910205	16.5322217
5)	8.3716425	2.3055518	2.8363484	16.0422414
6)	8.0586156	1.6751876	3.5614937	12.8514342
7)	7.9140421	1.0677454	4.8263259	12.2567512
8)	8.1199618	0.3039232	7.2648240	9.1066186

3.2 Statistics of nearest neighbor distance

The distance between particles is important in our study. We examined the nearest neighbor distance among groups (each has 512 points). A randomly distributed finite number of points in a finite range of space can be described by the theory of "point process". In general, the locations of particles in a field follows a Poisson process. The main objective of this section is to verify that the general theorem of nearest neighbor distance holds for particles in a turbulence field with/without random walks. The probability density function of the nearest neighbor distance r for the three dimensional case has the following form (Stoyan, Kendall and Mecke, 1987, p49).

$$f(r) = 3\lambda k r^2 \exp[-\lambda k r^3]$$

where $k = 4\pi/3$ and λ is the intensity of poisson process. For a known number of points n and finite volume σ, the value can be expressed

$$\lambda = n/\sigma$$

We used the box size of $(2\pi)^3$ for the simulation and each group contains 512 points. Thus

$$\lambda = 512/(2\pi)^3$$

The expected value of r can be expressed

$$E[r] = \int r f(r) dr$$

$$= (\lambda k)^{-1/3}\Gamma(4/3)$$

$$= 0.4354$$

If the particles follow the general Poisson process, the average value of nearest neighbor distance should agree with the above value and the average value should not depend on whether it is with a random walk or a pure turbulent motion. We started with the particles randomly distributed (uniform distribution) in space for each case. The statistics of nearest neighbor were calculated at every 10 th step. Not only the average values (solid line) but the standard deviation (broken line), the minimum (triangle) and the maximum (circle) did not change from the beginning to the end for all cases (Figure 1). This confirms that particles as a point process among the same group follow the stationary Poisson process.

4. Auto-Regressive models

It is desirable to find a usable stochastic model for the turbulence velocity field to implement various types of motion of an organism in difference environments. The successful model would enable us to reduce the amount of computation and to consider larger ranges of spatial scales. We are not looking for a "perfect" turbulence field but rather one that mimics the statistics as far as particle encounters are concerned. This result would make simple modelling schemes available to a large number of biological modelers.

A conventional approach to model the turbulence velocity field is Langevin's equation which has a form of first order stochastic differential equation. A discrete form of the equation can be expressed as a first order discrete AR process. Many attempts have been made to simulate turbulence, particularly for turbulent diffusion. Although many authors claim the simulations give reasonably good agreement with the observations, they have not tested the model against the real turbulent velocity data. We attempted to fit many different orders of AR processes to the velocity data. Two criteria were used to identify the best fit to a given data. AIC is the most common order criterion (Akaike, 1971) but seems to give higher order than the true process (Priestley, 1981). Another criterion used is LIL (Hannan and Quinn, 1979) and seems to give better results.

Table 4.1 (AIC) and 4.2 (LIL) show the number of best order fitted to velocity component u for the eight different cases. Case 1 (no random walk) appeared higher AR models to fit the data than what we initially expected. However, this can be explained from the following reason. Suppose the turbulence velocity field is in a class of second order stochastic equation, the discrete data from such kind of continuous process tend to appear as Autoregressive/moving average process of order (2,1) (ARMA(2,1)). Since we are trying to fit AR model to ARMA process we should expect a high order of AR model for the estimate. The result suggests that Langevin's equation (discrete form, so AR(1)) does not describe the velocity field well. The model may fit reasonably to the observed diffusion data but this may be an artifact of a statistical nature.

As far as the finding the best model for the turbulence velocity field concerns that we should consider fitting ARMA models but we have not a chance to perform a test.

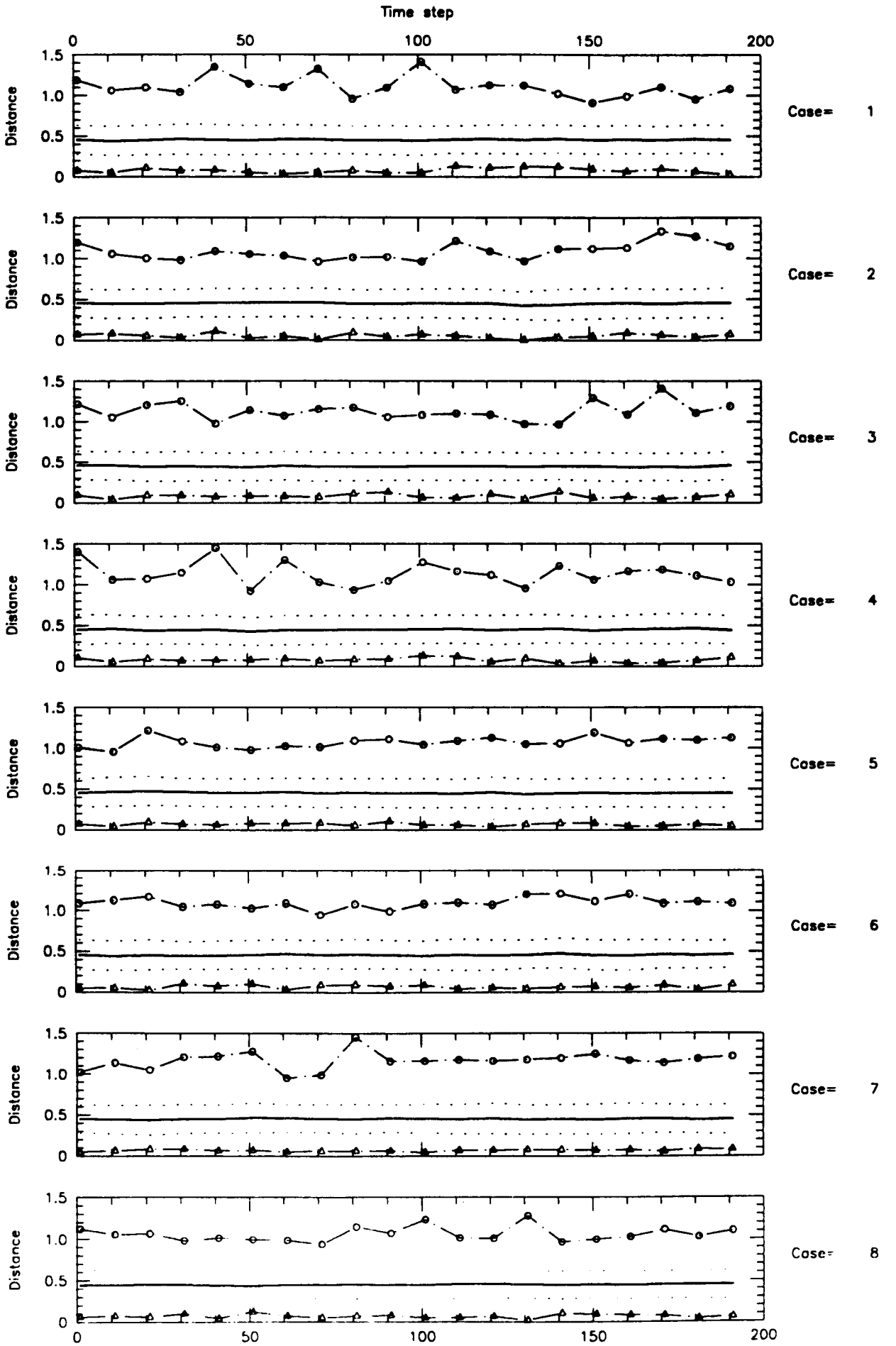
Time step
0
50
100
150
200
Distance
1.5
1.0
0.5
0
Case= 1
Case= 2
Case= 3
Case= 4
Case= 5
Case= 6
Case= 7
Case= 8

Fig. 1

Table 4.1 The number of best AR order by AIC. The data is velocity component u.

case	1	2	3	4	5	6	7	8
1th order # of aic=	0	0	104	216	241	231	262	325
2th order # of aic=	0	4	37	57	59	63	80	85
3th order # of aic=	0	8	20	32	38	44	47	37
4th order # of aic=	3	4	32	40	35	34	27	10
5th order # of aic=	1	6	29	31	24	38	21	11
6th order # of aic=	3	4	34	19	19	20	22	12
7th order # of aic=	3	8	29	20	16	16	8	7
8th order # of aic=	16	43	39	19	11	17	13	7
9th order # of aic=	20	37	22	10	11	13	9	4
10th order # of aic=	30	68	29	16	10	12	6	3
11th order # of aic=	49	71	26	11	7	8	5	2
12th order # of aic=	66	78	22	11	8	5	3	2
13th order # of aic=	81	60	27	8	14	5	2	3
14th order # of aic=	95	50	32	9	10	2	1	0
15th order # of aic=	29	24	9	7	9	2	5	3
16th order # of aic=	15	10	4	2	0	1	0	0
17th order # of aic=	10	2	4	1	0	0	0	0
18th order # of aic=	15	12	2	0	0	1	0	1
19th order # of aic=	9	4	1	0	0	0	0	0
20th order # of aic=	11	4	0	1	0	0	0	0
21th order # of aic=	12	6	3	0	0	0	1	0
22th order # of aic=	12	1	2	0	0	0	0	0
23th order # of aic=	9	5	2	1	0	0	0	0
24th order # of aic=	11	0	1	0	0	0	0	0
25th order # of aic=	6	2	1	0	0	0	0	0

Table 4.2 The number of best AR order by LIL. The data is velocity component u.

case	1	2	3	4	5	6	7	8
1th order # of lil=	0	1	229	366	390	384	395	434
2th order # of lil=	0	11	58	51	58	64	72	56
3th order # of lil=	2	14	22	27	21	24	25	13
4th order # of lil=	8	5	36	21	18	10	8	3
5th order # of lil=	1	9	38	22	10	11	4	3
6th order # of lil=	4	19	25	6	5	4	4	1
7th order # of lil=	15	37	25	5	5	3	0	1
8th order # of lil=	38	94	31	7	1	7	1	1
9th order # of lil=	41	49	9	1	2	3	2	0
10th order # of lil=	47	77	13	1	1	0	0	0
11th order # of lil=	68	59	9	2	0	2	0	0
12th order # of lil=	68	61	7	0	0	0	0	0
13th order # of lil=	64	28	4	0	0	0	0	0
14th order # of lil=	56	22	3	2	0	0	0	0
15th order # of lil=	33	12	3	1	1	0	0	0
16th order # of lil=	20	6	0	0	0	0	0	0
17th order # of lil=	8	1	0	0	0	0	0	0
18th order # of lil=	10	3	0	0	0	0	1	0
19th order # of lil=	7	2	0	0	0	0	0	0
20th order # of lil=	6	0	0	0	0	0	0	0
21th order # of lil=	4	1	0	0	0	0	0	0
22th order # of lil=	5	0	0	0	0	0	0	0
23th order # of lil=	4	1	0	0	0	0	0	0
24th order # of lil=	0	0	0	0	0	0	0	0
25th order # of lil=	2	0	0	0	0	0	0	0

References

Akaike, H., Information theory and an extension of the maximum likelihood principle. Research Memorandum N. 46, Institute of Statistical Mathematics, Tokyo. Published in 2nd Int. Symp. on Inf. Theory (Eds. B.N. Petrov and F. Csaki), 267-281. Akademiai Kiade, Budapest (1973). 1971

Hannan, E.J. and B.G. Quinn, The determination of the order of an autoregression, J. Roy. Statist. Soc., 38, 205-248, 1979.

Rothschild, B.J. and T.R. Osborn, Small-scale turbulence and plankton contact rates, J. Plankton Res., in press, 1988.

Stoyan, D., W.S. Kendall and J. Mecke, Stochastic geometory and its applications, John Wiley & Sons, New York, 1987.

Review of the Literature on Lagrangian modelling

There exists an abundant volume of literature about the Lagrangian method in the field of fluid dynamics. Much is based on theoretical works. A limited number of laboratory experiments have been conducted by actually tracing a particle in space. Jones et al. (1967) made an early experiment to study the three-dimensional motion of particles. Sullivan (1971) and Snyder and Lumley (1971) made similar experiments, while more recently Well and Stock (1983) and Sato and Yamamoto (1987) used an optical device to trace a particle in three dimension.

Numerical simulations have been applied in turbulence studies. The Lagrangian statistics are usually studied with "random walk" or Markovian processes. In his early paper on Lagrangian variables, Obukhov (1959) suggested that the evolution of a diffusion process can be described by a Markov process and obeyed the Fokker-Planck equation. The Langevin equation (Krasnoff and Peskin, 1971; Smith, 1968; Gifford, 1982) has been adapted to turbulent diffusion problems. Numerical simulations based on the Langevin equation were conducted by Reid (1978) and Hanna (1979). Ratm and Svensson (1986) applied the Langevin equation to oceanic diffusion within the Ekman layer, and obtained agreements with field observations of dispersion. Although simulation and observations show reasonable agreement, the Lagrangian auto-correlation function of velocity was in a form of an exponential function, and this constrains certain classes of turbulence from following the Langevin equation, particularly at low Reynolds number.

Random-walk theory has been used in this study of animal motions, as early as Patlak (1953a,b). Fraenekl and Gunn (1961) classified undirected response (kineses) into orthokinesis (modulation of velocity) and klinokinesis (modulation of turning rates). Rohlf and Davenport (1969) discussed the effect of a stimulus field on animal movement pattern. Doucet and Drost (1985) categorized the movement in depth. Terrestrial animal (insect) movements have been conjugated with the population dynamics (Jones, 1977). Kareiva and Shigesada (1983) extended the model to the first order Markov process. Siniff and Jessen (1969) examined the movement of red foxes and showed that the mean speeds associated with each path follow the gamma distribution. The distribution of turning angles appeared to be normally distributed. Equivalent aquatic observation have not been reported in the literature. Sakai (1973) is the only study, at least known to the authors, on a simulation of fish grouping. The model is developed from the dynamic equation of motion with "forces" including forward thrust, mutual interaction and arrayal forces, but the random forcing term is rather deterministic. The simulated grouping pattern shows amoebic, toroid and rectilinear movements.

Purcell (1977) and Zaret (1980) discuss the physical environment of planktonic organisms. In general the organisms live in highly viscous conditions at low Reynolds number. The population, however, is subject to turbulent diffusion and stirring. Accumulating evidence shows that planktonic food webs are strongly related to turbulent mixing (Sonntag and Parsons, 1979; Gallegos and Platt, 1982; McGowan and Hayward, 1978). Sverdrup (1953) defined the concept of critical depth for the relationship between mixing layers and phytoplankton growth. Numerical model studies were conducted by applying Eulerian type of equations (e.g. Tett, 1981). Recent review papers by Denman and Powell (1984) and Tell and Edwards (1984) discuss the effects of physical processes on planktonic organisms. Denman and Powell (1984) note that the relation of physical process and planktonic ecosystem should be studied by matching both biological and physical scales. By this account not only measurements of a planktonic

ecosystem but the modeling should be performed at the same order of scale. Eulerian types of models are based on averaged values over a certain physical scale, which is usually much larger than the size of the plankton. Tett and Edwards (19) mention that "Conversely, selection may operate to ensure that 'the plankton' tends always to exploit the available resources, and in this case continuum model (Eulerian model) might be adequate for predicting total biomass and production..". But they point out the Eulerian models are not suitable for studying the transient state and individual species of plankton. Then a Lagrangian model should be adopted. Lewis et al. (1984) apply an Eulerian model to study the mixing and photadaptation of phytoplankton, in which they claim that the Eulerian equations can be transformed into a Lagrangian coordinate system (they refer to Hill, 1976). This is "mathematically" true, but it is not tractable to obtain the Lagrangian statistics.

Since the Lagrangian models track each individual particle (or plankter), extensive computational effort is required. But recent rapid advancements in computer technology decreased the cost of computer operation drastically. A numerical simulation model of Ledbetter (1979) is the earlier attempt of the Lagrangian model to study plankton patchiness in the Langmuir circulations. Similar numerical experiment (Watanabe and Harashima, 1986) shows good agreement of the Lagrangian model with the aggregating pattern with the Langmuir circulation observed in a laboratory tank. Falkowski and Wirick (1981) use simple "random walk" to trace phytoplankton motion in the mixing layer. Woods and Onken (1982) use "random walk" plus sinusoidally modulated motion to study the effect of diurnal variation of mixing layers on the phytoplankton production. They follow a single plankter and run the same simulation 100 times to get an ensemble average of the plankton motion. Therefore the plankters are statistically and physically independent. Wolf and Woods (1987) extend Woods and Onken's model (1982) to investigate further the effects of diurnal and seasonal variation of mixed layer depth on phytoplankton production. They suggest that at least 20 particles in each one-meter depth interval over the entire mixed layer, 5000 particles for their case, are necessary to ensure a statistically significant result. They show that physiological adaptation of plankton depends on the history of their individual trajectory. A hybrid Lagrangian model with a two-layer mixed layer model (Eulerian) examines the sinking characteristics of planktonic organism (Lande and Wood, 1987).

References

Denman K.L. and T.M. Powell, Effects of physical processes on planktonic ecosystems in the coastal ocean, Oceanogr. Mar. Biol. Ann. Rev, 22, 125-168, 1984.

Doucet, P.G. and N.J. Drost, Theoretical studies on animal orientation II. Directional displacement in kineses, J. Theor. Biol., 117, 337-361, 1985.

Falkowski, P.G., C.D. Wirick, A simulation model of the effects of vertical mixing on primary productivity, Mar. Biol., 65, 69-75, 1981.

Fraenkel, G.S. and D.L. Gunn, The orientation of animals - kineses, Taxes and Compass Reactions, New York: Dover, 1961.

Gallegos, C.L. and T. Platt, Phytoplankton production and water motion in surface mixed layers, Deep-sea Res., 29, 65-76, 1982.

Gargett, A.E., T.R. Osborn and P.W. Nasmyth, Local isotropy and the decay of turbulence in a stratified fluid, J. Fluid Mech., 144, 231-280, 1984.

Gifford, F.A., Horizontal diffusion in the atmosphere: A Lagrangian-dynamical theory, Atmospheric Environment, 16, 505-512, 1982.

Hanna, S.R., Some statistics of Lagrangian and Eulerian wind fluctuations, J. Appl. Met., 18, 518-525, 1979.

Hill, J.C., Homogeneous turbulent mixing with chemical reaction, Ann. Rev. Fluid Mech., 8, 135-161, 1976.

Jones, B.G., B.T. Chao, M.A. Shirazi, Developments in Mechanics, Proc. 10th Midwestern Mech. Conf., Colorado State University, ed. J.E. Cermak, J.R. Goodman, 4, 1249-74, Fort Collins: Johnson Pub. Co., 1967.

Jones R., Movement patterns and egg distribution in cabbage butterflies, J. Anim. Ecol., 46, 629-642, 1977.

Kareiva, P.M. and N. Shigesada, Analyzing insect movement as a correlated random walk, Oecologia, 56, 234-238, 1983.

Krasnoff, E. and R.L. Peskin, The Langevin model for turbulent diffusion, Geophys. Fluid Dynam., 2, 123-146, 1971.

Lande, R. and M. Wood, Suspension times of particles in the upper ocean, Deep-sea Res., 34, 61-72, 1987.

Ledbetter, M., Langmuir circulations and plankton patchiness, Ecol. Model., 7, 289-310, 1979.

Lee, M.J. and W.C. Reynolds, Numerical experiments on the structure of homogeneous turbulence, Report No. TF-24, Depart. Mechanical Engineering, Stanford University, 1985.

Lewis, M.R., J.J. Cullen and T. Platt, Relationships between vertical mixing and photoadaptation of phytoplankton: similarity criteria, Mar. Ecol. Prog. Ser., 15, 141-149, 1984.

McGowan, J.A. and T.L. Hayward, Mixing and oceanic productivity, Deep-sea Res., 25, 771-793, 1978.

Obukhov, A.M., Description of turbulence in terms of Lagrangian variables, Adv. Geophys., 6, 113-116, 1959.

Okubo, A., Fantastic voyage into the deep: marine biofluid mechanics, Proc. Inter. Sym. Math. Biol., ed. E. Teramoto and M. Yamaguchi, Lecture note in Biomath., Springer-Verlag, 1986.

Patlak, C.S., Random walk with persistence and external bias, Bull. Math. Biophys., 15, 311-338, 1953a.

Patlak, C.S., A mathematical contribution to the study of orientation of organism, Bull. Math. Biophys., 15, 431-476, 1953b.

Purcell, E.M., Life at low Reynolds number, Amer. J. Phys. 45, 3-11, 1977.

Rahm, L., U. Svensson, Dispersion of marked fluid elements in a turbulent Ekman Layer, J. Phys. Oceanogr., 16, 2084-2096, 1986.

Riley, G.A., Theory of food chain relations in the ocean, The sea vol.2, 1963.

Robertson, S.B. and B.W. Frost, Feeding by an omnivorous planktonic copepod Aetideus divergens Bradhold, J. Exp. Mar. Biol. Ecol., 29, 231-244, 1977.

Rohlf, F.L. and D. Davenport, Simulation of simple model of animal behavior with a digital computer, J. theor. Biol., 23, 400- , 1969.

Reid, J.D., Markov chain simulations of vertical dispersion in the neutral surface layer for surface and elevated releases, Boundary-Layer Meteorology, 16, 3-22, 1979.

Sakai, S., A model for group structure and its behavior, Biophysics, 13, 82-90, 1973 (in Japanese).

Sato, Y. and K. Yamamoto, Lagrangian measurement of fluid-particle motion in an isotropic turbulent field, J. Fluid Mech., 175, 183-199, 1987.

Siniff, D.B. and Jessen C.R., A simulation model of animal movement patterns, Adv. Ecol. Res., 6, 185-219, 1969.

Smith, F.B., Conditioned particle motion in a homogeneous turbulent field, Atmospheric Environment, 2, 491-508, 1968.

Snyder, W.H. and J.L. Lumley, Some measurements of particle velocity auto correlation functions in a turbulent flow, J. Fluid, Mech., 48, 41-71, 1971.

Sonntag, N.C. and T.R. Parsons, Mixing an enclosed, 1300m^3 water column: effects on the planktonic food web, J. Plankton Res., 1, 85-102, 1979.

Sullivan P.J., J. Fluid Mech., 49, 551-76, 1971.

Sverdrup, H.U., On conditions for the vernal blooming of phytoplankton, Journal du Conseil permanent pour l'exploration de la mer, 18, 287-295, 1953.

Tett, P., Modelling phytoplankton production at shelf-sea fronts, Phil. Trans. R. Soc. Lond. Ser. A, 302, 605-615, 1981.

Tett, P. and A. Edwards, Mixing and plankton: An interdisciplinary theme in oceanography, Oceanogr. Mar. Biol. Ann. Rev., 22, 99-123, 1984.

Ulanowicz, R.E. and T. Platt, eds., Ecosystem theory for biological oceanography, Can. Bull. Fish. Aquat. Sci., 213, 1-260, 1985.

Watanabe, M. and Harashima, A., Interaction between motile phytoplankton and langmuir circulation, Ecol. Modelling, 31, 175-183, 1986.

Wells, M.R. and D.E. Stock, The effects of cross trajectories on the dispersion of particles in a turbulent flow, J. Fluid Mech., 136, 31-62, 1983.

Wolf, K.U. and J.D. Woods, Lagrangian simulation of primary production in the physical environment - the deep chlorophyll maximum and nutricline, unpublished manuscript, 1987.

Woods, J.D. and R. Onken, Diurnal variation and primary production in the ocean - preliminary results of a Lagrangian ensemble model, J. Plankton Res., 4, 735-756, 1982.

Zaret, R.E., The animal and its viscous environment, Evolution and ecology of zooplankton communities, Special symposium vol.3 Amer. Soc. Limnol. Oceanogr., ed. W.C. Kerfoot, Univ. Press of New England, Hanoer, New Hampshire and London, England, 3-9, 1980.

APPENDIX 4

List of Advisory Committee Members

CTR ADVISORY COMMITTEE LIST

Dr. Dennis M. Bushnell
MS. 163
NASA/Langley Research Center
Hampton, VA 23665-5225

Dr. Marvin E. Goldstein
Chief Scientist, MS. 60-2
NASA\Lewis Research Center
Cleveland, OH 44135

Dr. Jack Herring
National Center for Atmospheric Research
1850 Table Mesa Drive
Boulder, CO 80303

Professor Paul A. Libby
Department of Mechanical Engineering
University of California, San Diego
La Jolla, CA 92093

Professor John L. Lumley
Sibley School of Mechanical & Aerospace Engineering
238 Upson Hall
Cornell University
Ithaca, NY 14853

Dr. James McMichael
AFSOR/NA
Bolling Air Force Base
Washington, D.C. 20332-6448

Professor Steven A. Orszag
D-307 Engineering Quadrangle
Princeton University
Princeton, NJ 08544

Professor Anatol Roshko
Aeronautics Department
Mail Code 105-0
California Institute of Technology
Pasadena, CA 91125

Dr. Robert E. Singleton
Director, Engineering Services Division
U.S. Army Research Office
P.O. Box 12211
Research Triangle Park, NC 27709-2211

Dr. Ronald Smelt
P.O. Box Ag
Watsonville, CA 95077

Dr. Michael J. Werle
Manager, Gasdynamics and Thermophysics
United Technologies Research Center
East Hartford, CT 06108 ,Dr. Werle

Dr. Robert Whitehead
Fluid Mechanics Branch - Code 1132
Office of Naval Research
800 North Quincy Street
Arlington, VA 22217-5000

Dr. Helena Wisniewski
Director, Applied & Computational Mathematics Program
DARPA
1400 Wilson Blvd.
Arlington, VA 22209

Ex Officio Members:

Dr. Randolph A. Graves, Jr.
Director, Office of Aerophysics
CODE RF
NASA Headquarters
Washington, D.C. 2054

Jack N. Nielson
MS 200A-1
NASA/Ames Research Center
Moffett Field, CA 94035